Journal of Environmental Chemical Engineering 10 (2022) 108148

Contents lists available at ScienceDirect

Journal of Environmental Chemical Engineering

journal homepage: www.elsevier.com/locate/jece

E-peroxone process of a chlorinated compound: Oxidant species, degradation pathway and phytotoxicity

Deysi Amado-Piña, Gabriela Roa-Morales *, Mayela Molina-Mendieta, Patricia Balderas-Hernández, Rubi Romero, Carlos E. Barrera Díaz, Reyna Natividad *

Environmental Chemistry and Chem. Eng. Lab., Centro Conjunto de Investigación en Química Sustentable CCIQS, UAEM-UNAM, Universidad Autónoma del Estado de México, UAEMex Carretera Toluca-Atlacomulco, Km 14.5, C.P. 50200 Toluca, Mexico

ARTICLE INFO

Editor: Despo Fatta-Kassinos

Keywords:
Electroperoxone
BDD
4-chlorophenol
Ozone
Perchlorate
Phytotoxicity

ABSTRACT

An electro-peroxone (EP) process was conducted in an up-flow bubble column reactor with BDD electrodes. The efficiency of the process was tested in the 4-Chlorophenol (4-CPh) mineralization and compared with that attained by single treatments like ozonation (O_3) and electro-oxidation (EO). At $[TOC]_o$= 56 mg·L^{-1}, pH_o= 7.0, T = 293 K, j = 0.06 A·cm^{-2}, t = 120 min, the oxidation power decreased in the following order EP>EO>O_3, and the TOC removed was, in the same order, 100%> 93%> 40%. The calculated synergy coefficient was 0.31, while the mineralization current efficiency percentage (MCE%) and the energy consumption (EC) were 12.24% and 11.48%, 2.84 and 2.31 kW·h^{-1}, for EP and EO, respectively. The germination percentage of *Lactuca sativa,* was 100%, 30% and 20%, at the end of EP, EO and O_3, respectively. This indicates that phytotoxicity, was only eliminated with EP. Based on the by-products, e.g. aromatic compounds (4-chlorocatechol, catechol, phenol, p-benzoquinone, hydroquinone) and carboxylic acids (maleic, formic, fumaric, succinic, oxalic, malonic and acetic acids) identified by UHPLC-UV/DAD and the changes of the concentration of chloride ion (Cl^-), hypochlorite, chlorite, chlorate and perchlorate, a reaction pathway was proposed for the 4-CPh mineralization by the E-peroxone process. It was demonstrated that under the studied conditions both, hydrogen peroxide and ozone, are produced during EO. At the end of EO, H_2O_2, carboxylic acids and perhaps persulfates, are responsible for the phytotoxicity of the solution.

1. Introduction

In the last decades, advanced oxidation processes (AOPs) have emerged as a plausible option to decontaminate water polluted with persistent and trace organic contaminants. Within AOP, peroxone is a relatively novel process that has been proven to intensify the mineralization of organic molecules and consists of the combination of ozone (O_3) and hydrogen peroxide (H_2O_2). In this process, a synergic effect on organic pollutants degradation is observed [1]. This synergy is mainly attributed to the reaction between O_3 and H_2O_2 that produces hydroxyl radicals ($HO^\bullet$) [2], which is a more powerful oxidant ($E^0 = 2.80$ V) than ozone and hydrogen peroxide alone, and thus can oxidize most organic molecules even at diffusion control limited rates [2]. Then, in a conventional peroxone process, both, ozone (O_3) and H_2O_2, are added to the system in order to produce $HO^\bullet$ via reaction 1,

$$H_2O_2 + O_3 \rightarrow O_2 + H^+ + O_2^{\bullet-} + HO^\bullet \quad (1)$$

Some disadvantages of the conventional peroxone process are that requires the external addition of hydrogen peroxide (H_2O_2) and that this is unsafe to handle, transport and store due to its reactivity. This has motivated the in-situ electro-generation of H_2O_2 in peroxone systems, and the resulting process has been named electro-peroxone (E-peroxone) [3].

In an E-peroxone system, O_3 is added in the same way as in a conventional peroxone process and reacts with the in-situ electro-generated H_2O_2 to produce $HO^\bullet$ (reactions 2–5) which can rapidly mineralize the organic pollutants [4]. An E-peroxone process is typically conducted in an electrolysis cell equipped with a cathode to electrochemically reduce the sparged O_2 to H_2O_2 and HO_2^-, according to reaction (2) [5] and (3) [6,7],

$$O_2 + 2H^+ + 2e^- \rightarrow H_2O_2 \quad (2)$$

$$O_2 + H_2O + 2e^- \rightarrow HO_2^- + OH^- \quad (3)$$

* Corresponding authors.
E-mail addresses: groam@uaemex.mx (G. Roa-Morales), rnatividadr@uaemex.mx (R. Natividad).

https://doi.org/10.1016/j.jece.2022.108148
Received 30 December 2021; Received in revised form 20 June 2022; Accepted 21 June 2022
Available online 24 June 2022

$$HO_2^- + O_3 \rightarrow HO^\bullet + O_2^\bullet + O_2 \quad (4)$$

$$2H_2O_2 + 2O_3 \rightarrow H_2O + 3O_2 + HO_2^\bullet + HO^\bullet \quad (5)$$

In this way, the E-peroxone (EP) process has been proven to intensify the mineralization of different pollutants in wastewater (see Table 1). There are in Table 1 summarized the reaction conditions and the organic compounds or effluents that have been treated by EP. The best results of each study in terms of TOC removal and oxidation power are also included. First of all, it can be observed in this table that the superiority of the EP process oxidation power, when compared to the individual processes like O_3 and EO, has been well established in the treatment of both, synthetic and real wastewater. The same cannot be said for ozonation and electro-oxidation, since there are some works where O_3 efficiency is higher than electro-oxidation [8,9], although this might be a reflection of the type of cell. The existing literature is dominated by the mineralization of solutions prepared with dyes and pharmaceuticals. In most of these works, the preferred cathodes are carbonaceous materials-based, especially Carbon black/Polytetrafluoroethylene (C-PTFE). This is not surprising since its ability to produce H_2O_2 by the oxygen reduction reaction (ORR, reaction 2) is well documented. Thus, the results shown in Table 1, suggest that the efforts to intensify further the E-peroxone process are mainly based on the use of different anodic materials to platinum. In the context of electrodes material, it has also been demonstrated that the E-peroxone process can be successfully conducted with BDD electrodes [10,11]. This material offers some advantages such as the production of hydroxyl radicals on the anodic surface by reaction 6, in addition to the ORR at the cathodic surface (reaction 2), the concomitant production of O_3 (reaction 7) [10] and relatively high Faradaic efficiency (31.7%) [5]. It is worth pointing out that with BDD electrodes, the production of hydrogen peroxide is also plausible via reaction 8,

$$BDD + H_2O \rightarrow BDD(HO^\bullet) + H^+ + e^- \quad (6)$$

$$3H_2O \rightarrow O_{3(g)} + 6H^+ + 6e^- \quad (7)$$

$$2BDD(HO^\bullet) \rightarrow 2BDD + H_2O_2 \quad (8)$$

The information in Table 1 suggests that as long as the cathode is of a carbonaceous material, the oxidation power is in the order of EP>EO, when the results are contrasted with O_3 though, the order of the oxidation power is EP>O_3 >EO, excepting the process conducted with BDD electrodes, in such a case the reported order is EP >EO>O_3.

The efficiency of the E-peroxone on mineralizing organic compounds depends on the production of the different involved oxidant species that in turn depends on different operating variables such as cell type, electrodes material, current density and pH. The chemical complexity of the process is increased by the type of organic molecule that can act as the precursor of other oxidant species, like oxychlorine anions.

It was the main objective of this work to establish and understand the distribution of species like O_3, O_2, H_2O_2, chloride and oxychlorine anions and relate them with the by-products and phytotoxicity of a chlorinated aromatic compound (4-chlorophenol, 4-CP) oxidation by three processes, ozonation, electro-oxidation (EO) and E-peroxone (EP).

4-chlorophenol (4-CPh) was elected since is a compound used in several industries, e.g. production of nylon, resins, antioxidants, plasticizers, dyes, drugs, oil additives, explosives, disinfectants and pesticides [18,19]. Furthermore, phenolic molecules have been assumed as model ones to assess the efficiency of different advanced oxidation processes and this is mainly due to their recalcitrant nature.

2. Methods and materials

2.1. Chemicals and reagents

4-chlorophenol (purity 99%), phenol (99.5%), p-benzoquinone

Table 1
Applications of E-peroxone.

Pollutant	Reaction conditions	Results	Reference
Chloramphenicol	Continuous flow cell (2 anodes and 2 cathodes), gas diffusion electrode Cathode: carbon-cloth Anode: Ti=IrSnSb-oxides plate $[TOC]_o$= 20 mg·L^{-1} $[Na_2SO_4]_o$= 0.05 M $[pH]_o$= 3 F_{O3}= 17.5 mg·min^{-1} j = 0.010 A·cm^{-2}	Mineralization: 63% Oxidation power: EP>O_3 >EO-H_2O_2	[9]
Acid Violet Dye	Filter Press cell, gas diffusion electrode Cathode: carbon-cloth Anode: Ti=IrSnSb-oxides plate $[TOC]_o$= 40 mg·L^{-1} $[Na_2SO_4]_o$= 0.05 M $[pH]_o$= 3 F_{O3}= 17.5 mg·min^{-1} j = 0.020 A·cm^{-2}	Decolorization: 100% Mineralization: 60% Oxidation power: EP>O_3 >EO-H_2O_2	[8]
Levofloxacin	Filter Press cell, gas diffusion electrode Cathode: carbon-cloth Anode: Ti=IrSnSb-oxides plate $[TOC]_o$= 20 mg·L^{-1} $[Na_2SO_4]_o$= 0.05 M $[pH]_o$= 3 F_{O3}= 14.5 mg·min^{-1} j = 0.020 A·cm^{-2}	Mineralization: 63% Oxidation power: EP>O_3 >EO-H_2O_2	[12]
Clofibric acid	Undivided cell Cathode: BDD Anode: BDD or Pt/Ti $[TOC]_o$= 5.6 mg·L^{-1} $[pH]_o$= 7.53 $[Na_2SO_4]_o$= 0.01 M F_{O3}= 10 mg·min^{-1}	Mineralization: 90% EP >EO>O_3 Perchlorates are produced at the BDD surface	[11]
Phenol	Continuous cell Cathode: BDD Anode: BDD $[TOC]_o$= 118 mg·L^{-1} $[pH]_o$= 3 $[Na_2SO_4]_o$= 0.05 M O_3 = *In situ* produced	Mineralization: 75% EP >EO>O_3	[10]
Phenol	Divided cell Cathode: C-PTFE Anode: Ni and Sb doped Tin oxide $[Ph]_o$= 200 mg·L^{-1} $[pH]_o$= 7.4 $[Na_2SO_4]_o$= 0.1 M j = 0.010 A·cm^{-2} F_{O3}= 10 mg·min^{-1}	Mineralization: 95% EP >EO	[13]
Leachate concentrates	Divided cell Cathode: CNTs/C-PTFE GDE (with Ni foam) Anode: Ti/SnO_2-Sb_2O_5 $[TOC]_o$= 246 mg·L^{-1} $[pH]_o$= 7.3 $[Na_2SO_4]_o$= 0.1 M	Mineralization: 80% Reduction of applied voltage through decreasing the cathode potential with CNTs	[14]
Dye Orange II	Undivided cell Cathode: C-PTFE Anode: Pt $[DYE]_o$= 200 mg·L^{-1} $[pH]_o$= 7.53 $[Na_2SO_4]_o$= 0.05 M F_{O3}= 10 mg·min^{-1}	Decolorization: 100% Mineralization: 96% EP>O_3 >EO	[6]
Marine Aquaculture wastewater	Flow-through cell Cathode: Ti plate Anode: Ti/RuO_2-IrO_2 plate $[COD]_o$= 24 mg·L^{-1} $[pH]_o$= 8	COD removal: 48% by EO, and 14% by EP EO>EP	[15]

(*continued on next page*)

Table 1 (*continued*)

Pollutant	Reaction conditions	Results	Reference
	F_{O3}= 17.5 mg·min^{-1} j = 0.005 A·cm^{-2}		
Ibruprofen	Cathode: carbon-PTFE Anode: Pt plate $[IBU]_o$= 20 mg·L^{-1} $[pH]_o$= 5.2 $[Na_2SO_4]_o$= 0.05 M F_{O3}= 10 mg·min^{-1}	Mineralization: 100% EP>O_3 >EO	[16]
Landfill leachate	Cathode: carbon-PTFE Anode: Pt plate $[TOC]_o$= 1650 mg·L^{-1} F_{O3}= 10 mg·min^{-1} $[pH]_o$= 8.07	Mineralization: 87% EP>Peroxone (H_2O_2 added) >O_3	[17]

(98.0%), acetic acid (99.0%), formic acid (99.0%), fumaric acid (99%), succinic acid (99.0%), maleic acid (99.0%), oxalic acid (99.0%), malonic acid (99.0%) and H_3PO_4 (85.7%), were purchased from Merck; 4-chlorocatechol (97%), hydroquinone (99%), catechol (>99%), sodium sulfate (99%) and sodium hydroxide ACS pellets (97%), were purchased from Sigma-Aldrich and resorcinol (>99%) from Meyer. Methanol and acetonitrile (HPLC ultra gradient solvent, 99.99%) and sulfuric acid (97.4%) were from Fermont. Other chemicals like Potassium Phosphate monobasic (99.0%) was from J. T. Baker and $ZnSO_4$•7 H_2O (> 99%) was from Hycel. Sodium chloride (Merk), sodium thiosulfate (98.5%, J. T. Baker), hydrochloric acid (37%, Fermont), potassium iodide (99%, Merk), potassium bromide (98.5%, J.T. Baker) and sodium acetate (99%, J.T. Baker), monobasic sodium phosphate (98%, Sigma), phosphoric acid (85%, Merck), hydrogen peroxide (30%, Fermont), potassium permanganate (99%, J.T. Baker), potassium indigo trisulfonate (Sigma Aldrich). All solutions were prepared with deionized water (Mill-Q system).

2.2. Removal of 4-CPh by ozonation, electro-oxidation, and E-peroxone processes

The removal of 4-CPh was studied under three different chemical environments, ozonation (O_3), electro-oxidation (EO) and E-peroxone (EP) processes. The basic experimental set-up consisted of a 1.5 L jacketed up-flow bubble glass column reactor (see Fig. 1). In the ozonation and E-peroxone processes, the bubble column reactor was continuously fed at the bottom and through a porous disc (0.2 mm pore size) with a mixture of O_3 and air, that was fed at 0.150 L·min^{-1} by means of a 0–0.2 L·min^{-1} flowmeter. Under these conditions, the O_3 was fed at 10 mg/min. This mixture came from an ozone generator (Pacific Ozone Technology generator). The excess of ozone in the outlet gas was decomposed by an ozone destructor, which converts ozone into oxygen rapidly and without emitting any toxic gases, such as carbon monoxide or carbon dioxide.

EO and EP treatments were conducted under galvanostatic conditions (0.06A•cm^{-2}), using a DC power supply. To do so, a pair of BDD electrodes (anode and cathode) separated 1 × 10^{-2} m from each other (BDD film supported on a niobium substrate) was placed in the reactor. The electrodes were purchased from CONDIAS. The surface area of each electrode was 50 cm^2 (length=20 ×10^{-2} m, width= 2.5 10^{-2} m).

In order to establish an adequate Na_2SO_4 concentration, the effect of this variable on 4-CPh concentration was studied over time during the EO process in the range of 0.025 – 0.1 M. The results are presented in the supplementary material as Fig. S1. Since the initial 4-CPh removal rate with 0.05 M Na_2SO_4 (2.1 mg·L^{-1}·min^{-1}) was very similar to that obtained with 0.1 M Na_2SO_4 (2.0 mg·L^{-1}·min^{-1}), and about twice that obtained with 0.025 M Na_2SO_4 (1 mg·L^{-1}·min^{-1}), it was decided to conduct all the experiments with 0.05 M Na_2SO_4.

All experiments were conducted by triplicate with 1.3 L of 4-CPh solution (100 mg• L^{-1}) and initial pH= 7.0 ± 0.05. The initial pH was adjusted with NaOH. pH was not buffered during the experiments and its evolution with reaction time was established. Temperature was kept constant at 20 ± 2 °C by circulating water through the jacket of the up-flow bubble column reactor.

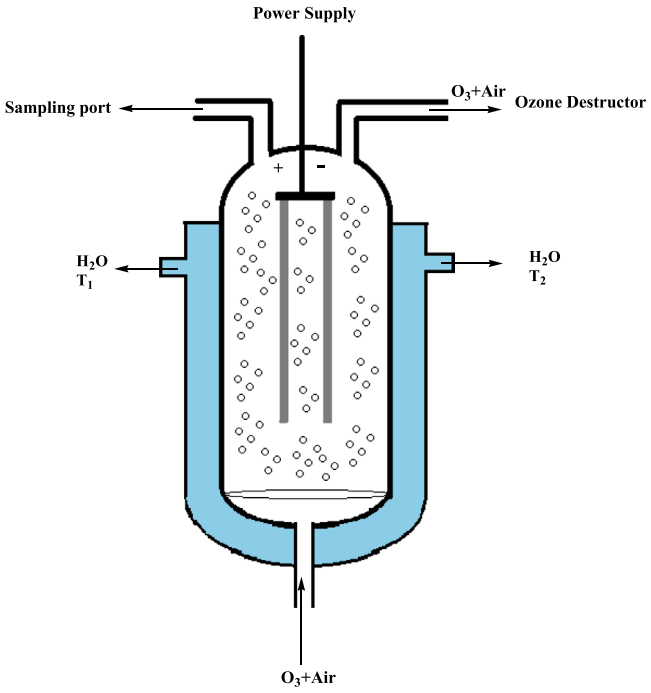

Fig. 1. Schematic of the reactor used for ozonation, electro-oxidation and E-peroxone treatment of 4-Chlorophenol.

2.3. Chemical Analysis

The concentration of 4-chlorophenol (4-CPh), p-benzoquinone (p-BQ), catechol, 4-chlorocatechol, phenol (Phe) and hydroquinone, was established by Ultra High Performance Liquid Chromatograph UHPLC (Vanquish, Thermo Scientific) equipped with an UV-Vis and PDA detector. The mobile phase (reversed-phase) was a mixture of 20% methanol, 80% water and 5 mM of H_2SO_4 at a flow rate of 1.0–1.3 mL• min^{-1}. An Ascentis ® Express C-18 (Supelco) column (3 cm × 4.6 mm and 2.7 μm) was used and the detection wavelength was 246 and 280 nm. The separation was achieved isocratically at 25 °C and the data analysis was performed using the software Chromeleon 7.

Carboxylic intermediates (e.g. oxalic, formic, fumaric, maleic, malonic, acetic acids), formed during the treatment, were measured using also the aforementioned Ultra High Performance Liquid Chromatograph (UHPLC). For this analysis, the mobile phase (reverse-phase) was a mixture of 3% methanol and 97% of monobasic potassium phosphate buffer (pH 2.3) with H_3PO_4. The flowrate of the mobile phase was 0.5 mL·min^{-1}. The injection volume was 5 μL. The identification wavelength was set at 210 nm. A reverse phase column Zorbax (Eclipse® XDB C-18, 15.0 cm in length and 4.6 mm in diameter, Agilent) was employed. Separation was isocratically achieved at 25 °C.

The dissolved oxygen was monitored using a Portable multiparameter pH meter, conductivity and dissolved oxygen (DO), HACH, HQ40d.

Hydrogen peroxide (H_2O_2) concentration profile was determined by a colorimetric method [20], using 3 mL of titanium sulfate (Ti^{4+}) reagent and 7 mL of sample. To prepare the titanium sulfate (Ti^{4+}) reagent, 1 g of TiO_2 was digested with 0.1 L of H_2SO_4 during 16 h in a thermal bath at 150 °C, the resulting solution was left to cool down and then it was diluted with four parts of water. The solution was then filtered with an asbestos material. The concentration of the titanium sulfate solution was 2000 mg·L^{-1}. The absorbance of samples was

determined by using a PerkinElmer Model Lambda 25 UV/Vis spectrophotometer and correlated to H_2O_2 concentration. The absorbance of samples was scanned from 200 to 900 nm and a maximum absorbance at 408 nm was observed. At this wavelength, the H_2O_2 extinction coefficient, $\varepsilon_{408\ nm}$, was 1715.4 $M^{-1}{\cdot}cm^{-1}$. The samples were scanned in a quartz cell with 1 cm optical path. The method is based on absorbance measurement of the color intensities of hydrogen peroxide solutions treated with titanium sulfate (Ti^{4+}) reagent. The yellow color produced in the reaction is due to the formation of pertitanic acid (reaction 9) [20],

$$Ti^{4+} + H_2O_2 + 2H_2O \rightarrow TiO_2{\cdot}H_2O_2 + 4H^+ \quad (9)$$

The ozone concentration was determined by a colorimetric method [21] using 10 mL of indigo reagent II and 90 mL of sample. The sample absorbance was determined at 600 nm with a PerkinElmer Model Lambda 25 UV/Vis spectrophotometer.

There are in Table S1, the limits of detection and quantification for the compounds determined by UHPLC, and other species like H_2O_2, O_3, DO, chlorides and TOC.

The concentration of chloride ions was measured by ionic chromatography (Aquion AS-DV, Dionex) with an AS11-HC- 4 μm x 250 mm column, the mobile phase (30 mM NaOH) was used at a flowrate of 1.5 mL·min^{-1}, the suppressor was manufactured by Dionex AERS 300 (4 mm × 480 mm x 121 mm), the current was 75 mA and the samples volume was 125 μL.

Total organic carbon (TOC) was measured using a TOC-L Shimadzu Total Organic Carbon analyzer in order to establish the mineralization of the initial solution. The pH was monitored using a Standard pH meter Meterlab (PHM210).

For the identification of oxychlorine anions, such as perchlorate, hypochlorite and chlorate, an iodometric method as reported in [22] was applied. For this purpose, 1 L of 0.01 N $Na_2S_2O_3$ solution was standardized by a potentiometric method [23].

In the identification of hypochlorite, the samples were treated with a pH= 4.2 acetate buffer, potassium iodide 10% and left to stand for 10 min in the dark. To determine the concentration of chlorates, the samples were treated with 500 mg of potassium bromide and 10 mL of HCl 10 M, then stirred constantly until complete dissolution. At this point, 10% potassium iodide was added, and it was allowed to stand for 10 min under complete darkness. The resulting solutions were then valorized with the standardized sodium thiosulfate solution through potentiometry.

For the perchlorate quantification, the total oxidation of the oxyanions to perchlorate was carried out with the addition of concentrated hydrochloric acid, later the 10% potassium iodide solution was added, the flask was covered and left to stand under complete darkness for 10 min. The resulting solution was then valorized by potentiometry with the standardized sodium thiosulfate solution [24].

For the potentiometric measurements, a Corning potentiometer was used. The reference and working electrode were of calomel and platinum, respectively. The involved reactions and equations to calculate the chloride and oxychlorine anions concentration are given in Section 4 of the supplementary material. The interference of H_2O_2 was eliminated as detailed also in Section 4 of the supplementary material.

2.4. Phytotoxicity tests

Twenty seeds of lettuce (*Lactuca sativa*) were placed in culture dishes (Petri dish) containing 5 mL of each sample, and then placed in an incubator at a constant temperature and darkness for 5 days (exposure time) for germination. The test procedure conditions are summarized in Table 2. Seed germination and the length of the longest root produced by the seeds were measured after 120 h. A visible root was used as the operational definition of seed germination. The percentages of relative seed germination (RSG) (Eq. 10), relative root growth (RRG) (Eq. 11) and the germination index (GI) (Eq. 12), were determined after exposure of the seeds with treated water as follows [25,26],

Table 2
Summary of seed germination test conditions.

Seed germination test (*Lactuca sativa*)	
Test type	Static
Temperature	22 °C± 2 °C
Light	No
Test vessel	Whatman No. 1 paper in a Petri dish
Test volumen	5 mL
Number of seeds	20
Replicates	3 for each sample
Positive control	Zn (II) ($ZnSO_4.7\ H_2O$) (25 mg·L^{-1} of Zn^{2+})
Negative controls	Deionized water and Na_2SO_4 (0.05 M)
Tested samples	Treatment time: 0, 5, 10, 20, 30, 45, 60, 75, 90, 105 and 120 min
Treatments applied to samples	Ozonation, Electro-oxidation and E-peroxone
Exposure time	120 h

$$RSG(\%) = \frac{\text{number of seeds germinated in the } \textit{sample}}{\text{number of seeds germinated in } \textit{the} \text{ control}} x100 \quad (10)$$

$$RRG(\%) = \frac{\text{mean root length in the } \textit{sample}}{\text{mean } \textit{root length} \text{ in control } \textit{sample}} x100 \quad (11)$$

$$GI(\%) = \frac{RSG\ x\ RRG}{100} \quad (12)$$

where,

GI (%) values near 0 indicate the toxicity or phytotoxicity is high or maximum (H).

GI (%) values below 50% indicate that toxicity is moderated (M).

GI (%) values near 100% indicate low or zero toxicity (L).

As can be seen in Table 2, three control experiments were also conducted, one with deionized water, another one with 0.05 M Na_2SO_4 solution and a positive control experiment with $ZnSO_4 7\ H_2O$ [27]. Three replicates of each control sample were prepared. The pH of controls was 7.0 ± 0.05.

3. Results and discussion

In order to enhance the understanding of the 4-chlorophenol degradation by E-peroxone process (EP), the reaction was also conducted under ozonation (O_3) and electro-oxidation (EO). For each process, the evolution with time profiles of pH, O_3, O_2 and H_2O_2, chlorite and oxychlorine species, were established without and with the organic pollutant. The intermediate compounds for each process were also established. Hence, herein the results attained with each process are separately presented and discussed. Only the toxicity results and chlorine species concentration values for the three processes are contrasted and discussed in one single section.

3.1. Ozonation

Fig. 2 shows the pH, O_3, O_2 and H_2O_2 temporary profiles during the ozonation process of a blank system (2a) (only water) and a 4-CPh solution (2b). Regarding pH, it can be observed that it is practically constant at about 6.5 during the whole ozonation of the blank system unlike the ozonation of the 4-CPh solution (Fig. 2b), where a practically immediate decrease is observed when the reaction system is fed with ozone. In Fig. 3a, it can be observed that some acids, like oxalic and maleic, appear from the first 5 min and therefore, these are responsible for the pH decrease observed in Fig. 2b, from 7.0 to about 4.5 in the first 5 min of reaction and then a further decrease down to pH 3.0 at around 20 min, when other carboxylic acids started to accumulate (i.e. formic, maleic, fumaric and succinic acids, see Fig. 3b). This pH= 3.0 did not

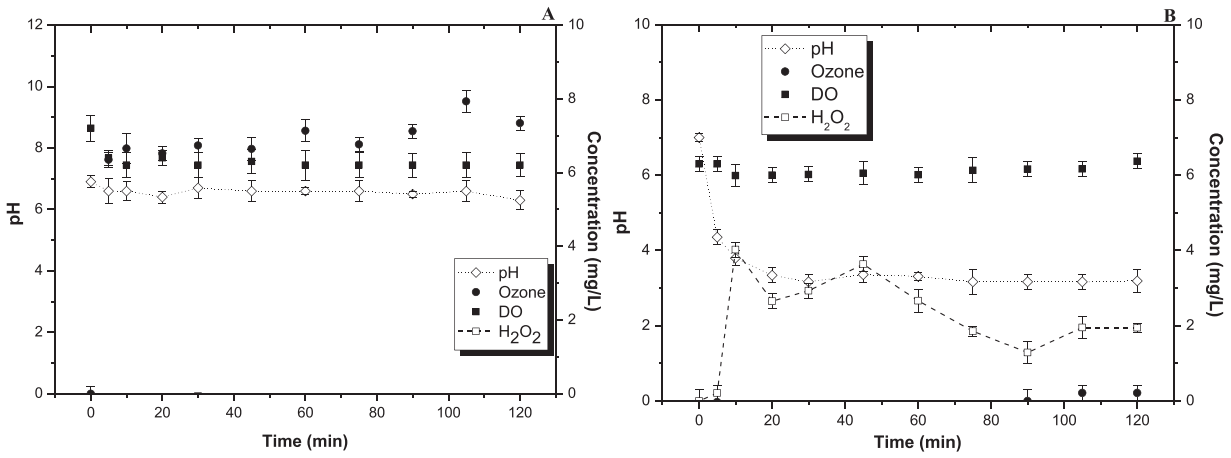

Fig. 2. Evolution with time of pH, dissolved ozone, dissolved oxygen (DO) and H_2O_2 during ozonation of (a) blank system: $[Na_2SO_4]$= 0.05 M, $[4\text{-CPh}]_o$ = 0.0 mgL^{-1} and (b) 4-Chlorophenol solution: $[Na_2SO_4]$= 0.05 M, $[4\text{-CPh}]_o$ = 100 $mg{\cdot}L^{-1}$. Constant reaction conditions: V = 1.3 L, F_{O3} = 10 mg/min, T = 20 ± 2 °C, pH_o= 7.0 ± 0.05.

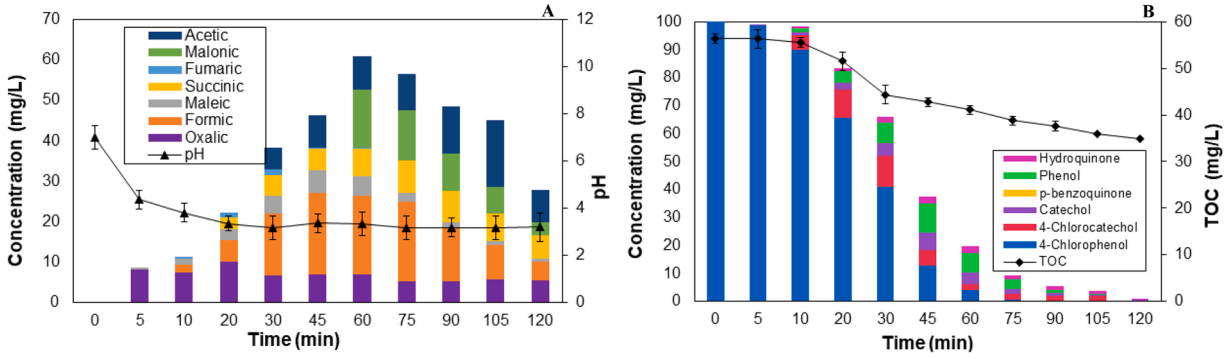

Fig. 3. Effect of ozonation on distribution of: a) carboxylic acids and pH, b) aromatic compounds and TOC during 120 min of treatment. *Reaction conditions:* $[Na_2SO_4]$= 0.05 M, $[4\text{-CPh}]_o$ = 100 $mg{\cdot}L^{-1}$, V = 1.3 L, F_{O3} = 10 mg/min, T = 20 ± 2 °C, pH_o= 7.0 ± 0.05.

change further in the rest of the experiment.

In ozonation, two possible oxidation routes may be considered: the direct way, due to the reaction between the molecular ozone and the dissolved compounds; and the indirect way, due to the reactions between the radicals (i. e. hydroxyl radicals $HO^{\bullet}$) produced during the ozone decomposition and the dissolved organic compounds [4,28]. The direct oxidation by O_3 occurs under acidic conditions while the indirect oxidation occurs under alkaline conditions. The effect of pH over ozone decomposition was investigated by Poznyak (2006) [29] and demonstrated that ozone decomposition at pH 7 is negligible. By contrasting Figs. 2a and 2b, it can be observed that ozone is depleted when the 4-CPh molecule is added. Thus, it can be concluded that the 4-CPh oxidation is due to a direct attack of the ozone molecule. Such a mechanism not only leads to the relative fast cleavage of the aromatic ring to produce single bond carboxylic acids (Fig. 3a) but also to the concomitant production of hydrogen peroxide (Fig. 2b). After this time, H_2O_2 overall concentration gradually decreases and achieves a new plateau at a much lower concentration value (2 ppm). H_2O_2 can be assumed to be produced during the degradation of 4-CPh, mainly during the cleavage of hydroxylated aromatic compounds [30] and their further degradation into single bond carboxylic acids [31]. Actually, the period of time during which H_2O_2 concentration is the highest, between 10 and 60 min, coincides with a steeply decrease of 4-CPh concentration (Fig. 3b) and also with a positive sharp slope on carboxylic acids concentration, especially formic acid (Fig. 3a), while the accumulation of hydroxylated compounds does not seem to occur at the same rate. Fig. S2 shows the decrease in concentration of hydrogen peroxide combined only with ozone, without adding any organic molecule. It can be seen that, albeit at initial pH= 7.0, the decrease of H_2O_2 concentration only with O_3 is plausible. At acid pH, the removal of H_2O_2 is expected to be slower due to the H_2O_2 pKa. At this point is worth noticing, however, that has been previously reported the oxidation of carboxylic acids, like maleic and oxalic acid, with H_2O_2 and O_3 at initial pH as low as 2.2 [32], therefore the production of oxidant species when adding H_2O_2 and O_3, at acid pH, cannot be completely discarded.

It can also be observed in Fig. 3b that the removal of TOC by ozonation alone is only 40%. This can be mainly ascribed to the recalcitrant character of the remaining carboxylic acids, mainly oxalic and succinic acid. It is worth noticing that the concentration of oxalic and succinic acid does not significantly change over time. This indicates the hydroxyl radicals production is either non-existent or not enough to conduct the oxidation of such molecules [31] and confirms that the prevailing mechanism is the attack of the 4-CPh and the intermediate aromatic compounds (see Fig. 3b) by molecular ozone.

3.2. Electro-oxidation (EO)

Figs. 4a and 4b show the temporary profiles of dissolved ozone, oxygen, hydrogen peroxide and pH, during the electrolysis of a blank system and of a 4-CPh solution (Fig. 4b). There are significant differences between these two figures. To begin with, in the blank system, pH steeply increases from an initial value of 7 up to 10 in the first 45 min and then the rate of pH change slows down and increases only up to 11 in the last 75 min of electrolysis. This switch of pH can be ascribed to the reduction of water at the BDD cathode by means of the following reaction,

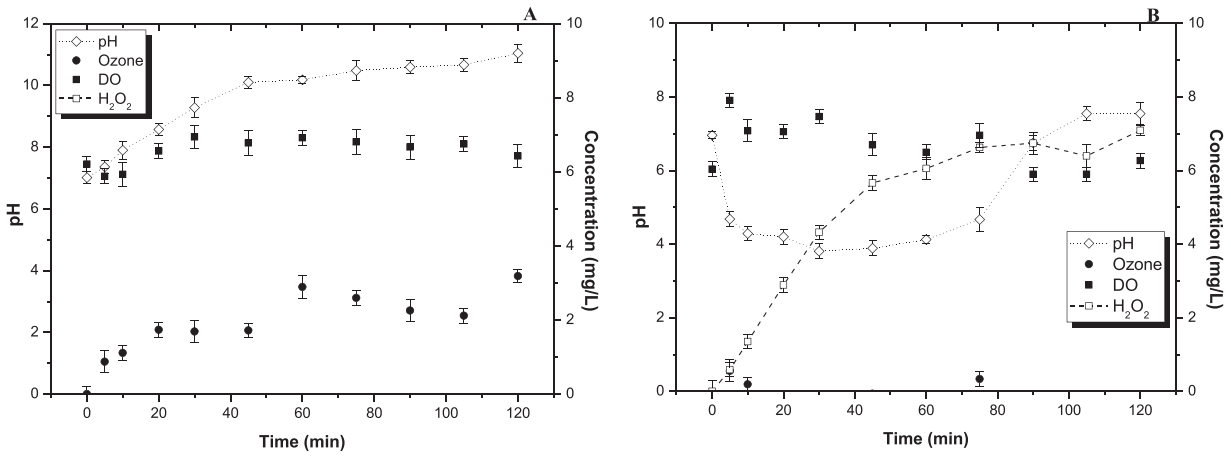

Fig. 4. Evolution with time of pH, dissolved ozone, dissolved oxygen (DO) and H_2O_2 during electro-oxidation of (a) blank system: $[Na_2SO_4]$= 0.05 M, $[4\text{-CPh}]_o$ = 0.0 mg·L^{-1} and (b) 4-Chlorophenol solution: $[Na_2SO_4]$= 0.05 M, $[4\text{-CPh}]_o$ = 100 mg·L^{-1}. Constant reaction conditions: V = 1.3 L, Q_{gas}= 0.150 L·min^{-1}, T = 20 ± 2 °C, pH_o= 7.0 ± 0.05, j = 0.060 A·cm^{-2}.

$$2H_2O + 2e^- \rightarrow 2HO^- + H_2 \quad (13)$$

It is also worth noticing that although ozone is not being fed into the system, this is detected during the electrolysis of the blank system albeit in small quantities (up to 3 ppm) produced by (reaction 6) and the BDD anode is responsible for this. Once the ozone is produced, this may participate further in other reactions that also contribute to the pH increase, i.e. reaction 14,

$$O_3 + H_2O + e^- \rightarrow HO^{\cdot} + O_2 + HO^- \quad (14)$$

This reaction may also be limiting the increase of ozone concentration. In addition, it should be kept in mind, that alkaline conditions promote ozone decomposition via de following reactions [33],

$$O_3 + OH^- \rightarrow HO_2^- + O_2 \quad (15)$$

$$O_3 + HO_2^- \rightarrow HO_2^{\bullet} + O_3^{\bullet -} \quad (16)$$

$$HO_2^{\bullet} \rightarrow O_2^{\bullet -} + H^+ \quad (17)$$

$$O_2^{\bullet -} + H^+ \rightarrow HO_2^{\bullet} \quad (18)$$

$$O_3 + O_2^{\bullet -} \rightarrow O_3^{\bullet -} + O_2 \quad (19)$$

$$O_3^{\bullet -} + H_2O \rightarrow HO^{\bullet} + O_2 + OH^- \quad (20)$$

$$O_3^{\bullet -} + HO^{\bullet} \rightarrow HO_2^{\bullet} + O_2^{\bullet -} \quad (21)$$

$$O_3 + HO^{\bullet} \rightarrow HO_2^{\bullet} + O_2 \quad (22)$$

$$HO_2^- + H^+ \rightarrow H_2O_2 \quad (23)$$

$$H_2O_2 \rightarrow HO_2^- + H^+ \quad (24)$$

$$O_3 + HO^{\bullet} \rightarrow O_3 + OH^- \quad (25)$$

Interestingly enough, the maximum ozone concentration is around 50% of that achieved in the ozonation system. As observed in Fig. 4b, the produced ozone, is totally consumed when the 4-CPh molecule is added. From the point of view of sustainability, these characteristics imprint to the electrolysis system an added value since not only allows to produce a highly oxidant molecule like ozone but also ensures the full use of it, thus eliminating the need of the ozone "destruction" stage. This also indicates that the analysis of an oxidation process should not be based only in the detected species during reaction but also on those produced when the chemical compound is not present, since the fact of not being observed during reaction might be because they are depleted rather than not produced, and therefore their participation in the reaction process should be taken into account.

In EO, the direct anodic oxidation of aromatic compounds has been demonstrated to occur in non-aqueous media [34]. In this case, although the direct anodic oxidation of 4-CPh could be expected, the extent of such a reaction may not be significant compared to the oxidation of water because this is in excess, and this fact may turn reaction 6 to be predominant. Thus, the oxidation of 4-CPh and its intermediates is expected to occur at the BDD anode but mainly via $HO^{\bullet}$ radicals. Although this is truth in many cases, here, the very first step of 4-CPh degradation is the molecular attack by ozone rather than by $HO^{\bullet}$ radicals. This is supported by the fact that pH and 4-CPh concentration decreased at very similar rates than did during the first 5 min of the ozonation process. This can be established by comparing Figs. 2b and 4b, 3b and 5b. The pH decline in the first 5 min of reaction from 7 to 4.5, can be ascribed, as in the case of ozonation, to the relatively fast production of carboxylic acids, mainly oxalic. It is worth pointing out a remarkable difference between ozonation and EO, that is the amount of accumulated carboxylic acids. By contrasting Figs. 3a and 5a, it can be concluded that this amount in the EO is less than half of that in the ozonation process. At this point is where the participation of the $HO^{\bullet}$ radicals is acknowledged since all acids rapidly disappear and actually succinic acid is fully oxidized unlike in the ozonation process. The oxidation of this acid is known to be conducted relatively fast by $HO^{\bullet}$ radicals [31].

Also, the TOC removal by EO was ~93% while in the ozonation was only 40% (Figs. 5b and 3b, respectively). It can also be observed in Fig. 5a, that the oxidation of carboxylic acids after 75 min is parallel to an increase in pH, which at the end of the process is about neutral (7.5). It is worth noticing that the dissolved oxygen is kept within 6–7 ppm during the whole EO process. It is rather important to keep enough dissolved oxygen, (DO) U.S. EPA > 4 mg·L^{-1} [35], in the water bodies and in those treated effluents, since low DO concentration can negatively affect the living organisms in the receiving water bodies.

Although there is some oxygen already dissolved in the water used to prepare the solution (see Fig. 4a), oxygen can also being produced by the following anodic reaction [36],

$$BDD(HO^{\cdot}) + H_2O \rightarrow BDD + O_2 + 3H^+ + 3e^- \quad (26)$$

The EO and EP processes were conducted with a 0.05 M Na_2SO_4 solution. This implies the presence of sulfate anions in the solution that are prone to be also oxidized at the anode either directly or by hydroxyl radicals and the result would be an also oxidant radical $(SO_4^{\cdot -})$, whose reactivity towards 4-CPh is comparable to that of $HO^{\cdot}$ [37], and therefore these species are also expected to participate in the 4-CPh oxidation. In this study and based on the observed pH during the whole treatment, the

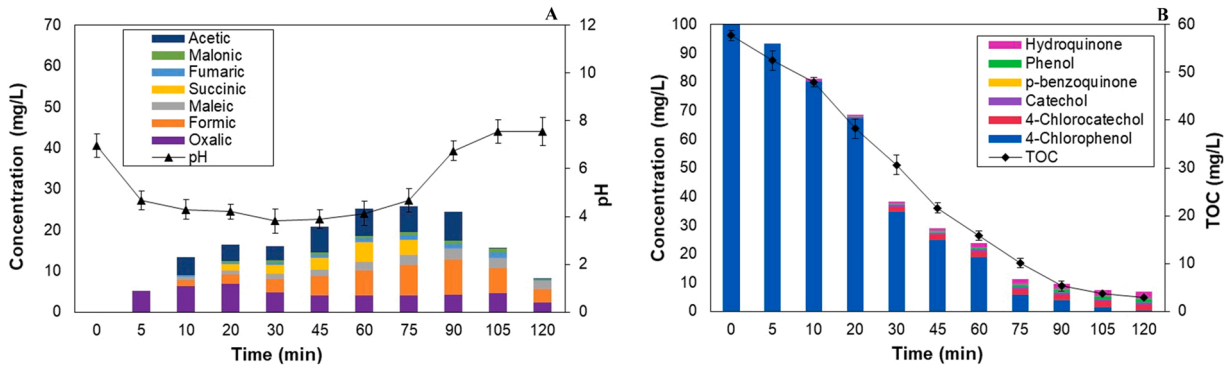

Fig. 5. Effect of electro-oxidation on distribution of: a) carboxylic acids and pH, b) aromatic compounds and TOC during 120 min of treatment. *Reaction conditions:* $[Na_2SO_4]$= 0.05 M, $[4\text{-CPh}]_o$ = 100 mg·L^{-1}, V = 1.3 L, Q_{gas}= 0.150 L·min^{-1}, T = 20 ± 2 °C, pH_o= 7.0 ± 0.05, j = 0.060 A·cm^{-2}.

expected oxidation of the sulfate anion may be occurring by reaction 27, since reaction 28 is favoured at pH lower than 1.99 [38].

$$SO_4^{2-} \rightarrow SO_4^{\bullet-} + e^- \quad E^\circ = 2.5\ a\ 3.1V \tag{27}$$

$$HSO_4^- + HO^\bullet \rightarrow SO_4^{\bullet-} + H_2O \quad k = 4.7x10^5\ M^{-1}s^{-1} \tag{28}$$

Once produced, the sulfate radicals can react between them and produce another oxidant specie, the persulfate anion ($S_2O_8^{2-}$) by reaction 29, or with water to produce hydroxyl radicals (reaction 30) [38],

$$SO_4^{\bullet-} + SO_4^{\bullet-} \longrightarrow S_2O_8^{2-} \quad k = 7.6x10^8\ M^{-1}s^{-1} \tag{29}$$

$$SO_4^{\bullet-} + H_2O \longrightarrow SO_4^{2-} + HO^\bullet + H^+ \quad k < 2.0x10^8\ M^{-1}s^{-1} \tag{30}$$

These reactions would be proceeding at the anodic surface. The excess of water, however, suggests that if there is a predominant reaction occurring at the BDD anode, that would be reaction 6.

3.3. Electro-peroxone (EP) treatment

The graphs in Fig. 6 show pH, dissolved oxygen (DO), ozone and H_2O_2 concentration as a function of time under electrolysis with BDD electrodes and constant flow of an ozone-air mixture. Like in the other treatments, the difference between Fig. 6a and Fig. 6b is that in the former, the solution initially contained only electrolyte while in the latter, 4-CPh was added. In Fig. 6a, pH, DO and H_2O_2 are observed to follow a rather similar trend and values to those in EO (Fig. 4a). Ozone concentration, however, is observed to attain a much higher value in this case (≈8.5 mg·L^{-1}) since the very beginning of treatment and this is due to the feeding of O_3 into the reactor. When 4-CPh is added to the system (Fig. 6b), ozone is depleted and H_2O_2 starts to accumulate since the first 5 min of reaction and unlike the H_2O_2 in EO, in this case presents a kind of Gaussian behaviour. This important difference can be considered the evidence of the E-peroxone process. In the case of EP, the maximum observed H_2O_2 concentration is ≈ 5.7 mg·L^{-1} at 30 min of treatment. Then this accumulated H_2O_2 is rapidly consumed at a rate of 0.14 mg·min^{-1} in the following 30 min. In the last 30 min of treatment, the system is observed to be H_2O_2 depleted thus limiting the hydroxyl radicals production rate via E-peroxone. Interestingly enough, in the same period of time, ozone starts to show again in the system, and this reinforces the suggestion of the occurrence of E-peroxone treatment. Because ozone was proven to be in situ produced during EO (Fig. 4a), a certain degree of EP cannot be disregarded during EO. This, however, occurs in less extent than when O_3 is constantly fed to the system (EP).

Unlike the other variables, pH profile is very similar for the three treatments during the first 60 min. Nevertheless, the lowest pH in both, EO and EP (about 3.5), is never as low as in the case of ozonation (pH_{min}=3.0). In EP, the lowest attained pH at 30 min coincides with the maximum concentration of carboxylic acids (see Fig. 7a). Its increase after this time can be ascribed to the removal of carboxylic acids, and it finally reaches a pH of 9.5, which is higher than that attained during EO. This is due to the presence of carboxylic acids after EO treatment (see Fig. 5a). The carboxylic acids profile during EP (Fig. 7a) also coincides with the H_2O_2 trend (Fig. 6b). The benefit of this process (EP) is evident in the achieved TOC removal. As can be seen in Fig. 7b, a complete mineralization is reached during EP while in EO the percentage of TOC

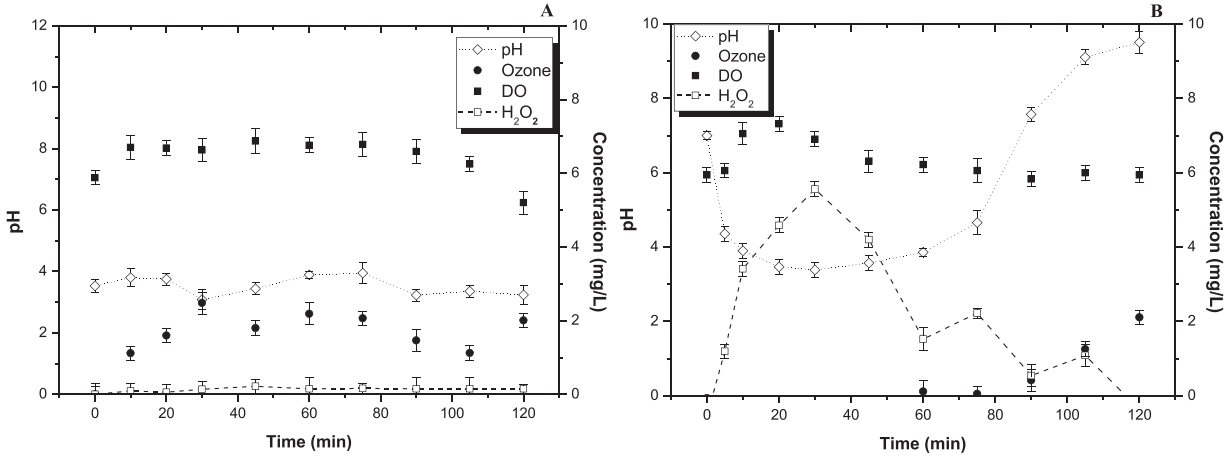

Fig. 6. Evolution with time of pH, dissolved ozone, dissolved oxygen (DO) and H_2O_2 during E-peroxone of (a) blank system: $[Na_2SO_4]$= 0.05 M, [4-CPh]o = 0.0 mg·L-1 and (b) 4-Chlorophenol solution: $[Na_2SO_4]$= 0.05 M, $[4\text{-CPh}]_o$ = 100 mg·L^{-1}. Constant reaction conditions: V = 1.3 L, F_{O3} = 10 mg/min, T = 20 ± 2 °C, pH_o= 7.0 ± 0.05, j = 0.060 A·cm^{-2}.

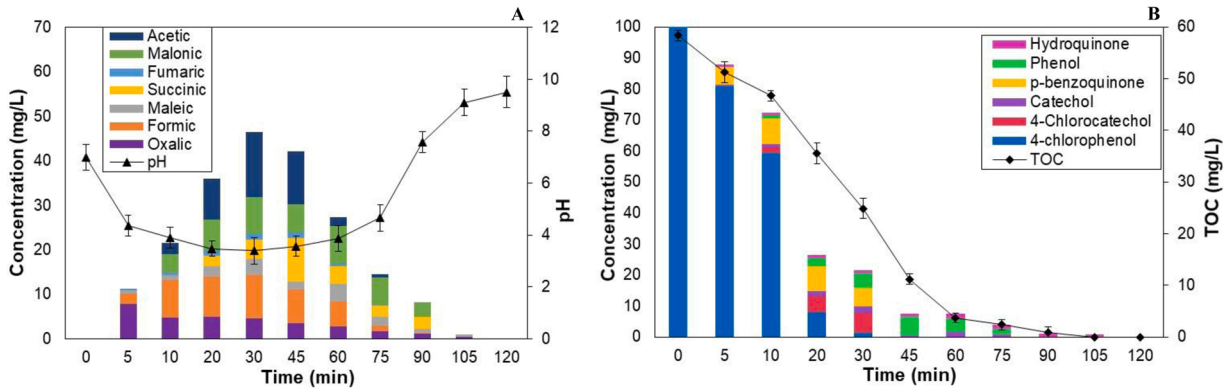

Fig. 7. Effect of E-peroxone treatment on distribution of: a) carboxylic acids and pH, b) aromatic compounds and TOC during 120 min of treatment. Reaction conditions: $[Na_2SO_4]$= 0.05 M, $[4\text{-CPh}]_o$ = 100 mg·L^{-1}, V = 1.3 L, F_{O3} = 10 mg/min, T = 20 ± 2 °C, pH_o= 7.0 ± 0.05, j = 0.060 A·cm^{-2}.

removed was 93% and in ozonation was 40%. It is also relevant to mention, that not only the mineralization extent was higher in the EP process than in the other two, but this value was also achieved at a lower time (105 min) than in the other two. The higher mineralization degree achieved during EP is partly responsible for the increase of pH since a higher concentration of CO_2 favours the production of carbonates (CO_3^{2-}).

It can be seen in Fig. S4, the 4-CPh concentration profiles under the three assessed treatments, at constant acid pH of 3.5 that was the lowest achieved during EP (Fig. 6b). As can be observed, also at constant pH, the removal rate of 4-CPh is higher during EP than in O_3 and EO.

In order to establish whether the removal of TOC in the EP process is the result of a synergic effect between O_3 and EO, the synergy coefficient between processes was calculated according to Eq. 31 [39],

$$S = \frac{k_{hybrid} - k_{individual}}{k_{hybrid}} \tag{31}$$

where S is the synergy coefficient and k is the kinetic constant. There are in Table 3, summarized the calculated values of the pseudo-first order kinetic constant for every individual process, O_3 or EO, and for the hybrid process, EP. These constants were obtained by plotting ln (TOC_o/TOC) vs reaction time for each process. As can be seen, the synergy coefficient is a positive value, and this is evidence of the synergic effect of O_3 and EO [39]. It is worth noticing that when conducting the experiments at constant pH= 3.5, the synergy coefficient was also positive. The results with constant pH= 3.5 are summarized in the supplementary material (Fig. S4 and table S4).

In addition, the percentage of mineralization current efficiency, MCE (%), and the energy consumption (EC) were also calculated according to Eq. 32 and 33, respectively.

$$MCE\left(\%\right) = \frac{nFV_s\Delta(TOC)_{Exp}}{4.32x10^7 mIt} \tag{32}$$

where n is the number of electrons involved in the complete oxidation of 4-CPh and that is 26 according to the following reaction,

$$C_6H_5OCl + 11H_2O \rightarrow 6CO_2 + Cl^- + 27H^+ + 26e^- \tag{33}$$

F is the Faraday constant and its value is 96,487 C·mol^{-1}, V_s is 1.3 L (solution volume), Δ(TOC) is the change in total organic carbon in mg·L^{-1}, the value of m is 6 and represents the number of carbons, I is the applied current in A, t is the electrolysis time in h and finally, the constant, 4.32 × 10^7, is a conversion factor.

The specific energy consumption per unit of TOC was calculated by means of,

$$EC\left(\frac{kWh}{g\ \ TOC}\right) = \frac{E_{cell}\cdot I\cdot t}{V_S\Delta(TOC)_{Exp}} \tag{34}$$

where E_{cell} is the mean cell voltage (V).

Table 4 presents the results obtained when applying Eq. 32 and 33 to each process, O_3, EO and EP. It is worth clarifying that in the case of O_3, the MCE (%) was not calculated because there is not an electrical current directly involved in the O_3 process. The value of EC shown in Table 4 for O_3, corresponds to the energy consumed during the production of O_3. Regarding the electrochemical processes, EO and EP, it can be observed that the lowest energy consumption was in the EP process. This can be ascribed to the already demonstrated synergetic effect of O_3 and EO in the EP process.

The EO of 4-CPh with BDD electrodes has been previously reported [40] albeit at higher current densities (0.25–0.4 A·cm-^{2}), higher initial 4-CPh concentration (500 mg·L^{-1}) and higher sodium sulfate concentration (0.1 M) than in this work. As consequence, the EC in such a work was also higher (2.6 kWh/TOC) than in this work (see Table 4). Regarding the MCE(%), the calculated value in this work, at the end of treatment, was 11.48% while in the above mentioned work was only 9%. The higher value of EC for EP is attributable to the energy consumption during the O_3 generation.

3.4. Production of chloride and oxychlorine anions during O_3, EO and EP

For each process, the chloride concentration was determined overtime. The measured chloride concentration was then contrasted with theoretical chloride values that were calculated under the assumption that the dichlorination of each mole of 4-CPh produces one mole of chloride [41]. In this way, the estimated theoretical chloride ions concentration was 35.89 mg·L^{-1} after 120 min of treatment. Fig. 8 depicts

Table 3
Pseudo-first order kinetic constants *(k)* for TOC removal and synergy coefficient (*S*) with ozonation (O_3), electro-oxidation (EO) and E-peroxone (EP) at pH_o= 7.0. R^2 =determination coefficient.

Treatment	R^2	k (min^{-1})	S
O_3	0.9728	0.0051	0.31
EO	0.9949	0.0247	
EP	0.9853	0.0430	

Table 4
Mineralization efficiency and Energy Consumption at the end of every treatment (120 min).

Process	MCE (%)	EC kWh/g TOC
Ozonation	–	0.47
EO	11.48	2.31
EP	12.24	2.84

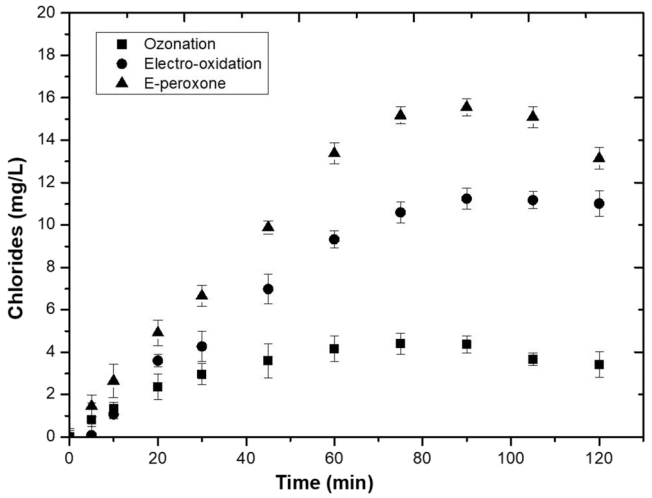

Fig. 8. Effect of treatment type and time on chlorides concentration: a) ozonation, b) Electro-oxidation (EO), c) Electro-peroxone (EP). Reaction conditions: $[Na_2SO_4]_o$= 0.05 M, $[4\text{-CPh}]_o$ = 100 mg·L-1, V = 1.3 L, j = 0.060 A·cm^{-2}, Q_{gas}= 0.150 L·min^{-1}, F_{O3} = 10 mg/min, T = 20 ± 2 °C, pH_o= 7.0 ± 0.05.

the chloride concentration as a function of treatment type and time. The attained maximum chloride concentration represented 57%, 41% and 16% of the theoretical value for EP, EO and O_3, respectively. This suggests that most of chlorine is not in an oxidized form in the case of EP process [42]. The maximum chlorides concentration varies according to the following order EP>EO> O_3.

As can be seen in Figs. 9–11, the distribution of other chlorine species also depends on the type of treatment. The plausible oxychlorine species produced upon oxidation of a chlorinated compound are hypochlorite (ClO^-), chlorite (ClO_2^-), chlorate (ClO_3^-), and perchlorate (ClO_4^-). Fig. 9 shows the oxychlorine anions distribution during ozonation. It can be observed that such a distribution is significantly different to that observed during EO and EP, Figs. 10 and 11, respectively. In the case of ozonation, the oxychlorine anion with the highest concentration is chlorate. This ion, according to Levanov, 2019 [43], can be produced by O_3 molecular attack and/or by hydroxyl radicals of chloride ions in solution, depending on pH. It can also be observed in Fig. 9, that the concentration of chlorate starts to decrease after 45 min of treatment. This can be associated to a plausible chlorate reduction by H_2O_2, that is being in-situ produced (see Fig. 2b) [44]. An increase in chlorate concentration is once again observed after 75 min and this can be ascribed

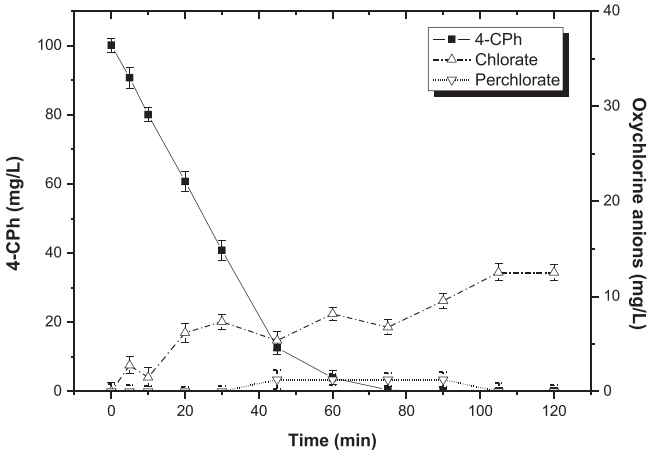

Fig. 9. Effect of ozonation on the temporary profiles of oxychlorine anions. *Reaction conditions:* $[Na_2SO_4]_o$= 0.05 M, $[4\text{-CPh}]_o$ = 100 mg·L^{-1}, V = 1.3 L, F_{O3} = 10 mg/min, T = 20 ± 2 °C, pH_o= 7.0 ± 0.05.

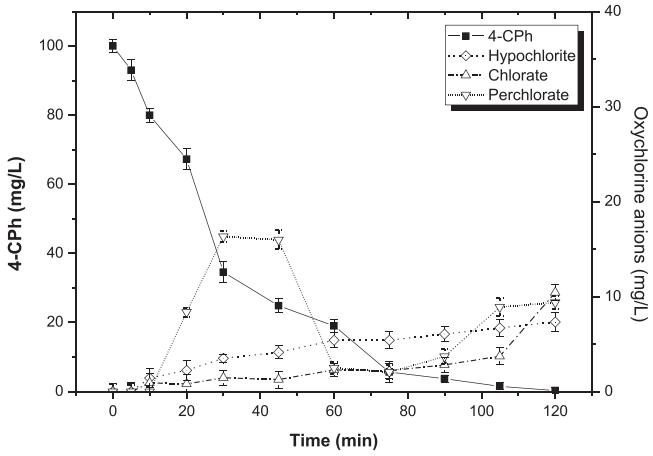

Fig. 10. Effect of Electro-oxidation on the temporary profiles of oxychlorine anions. *Reaction conditions:* $[Na_2SO_4]_o$= 0.05 M, $[4\text{-CPh}]_o$ = 100 mg·L^{-1}, V = 1.3 L, j = 0.060 A·cm^{-2}, Q_{gas}= 0.150 L·min^{-1}, T = 20 ± 2 °C, pH_o= 7.0 ± 0.05.

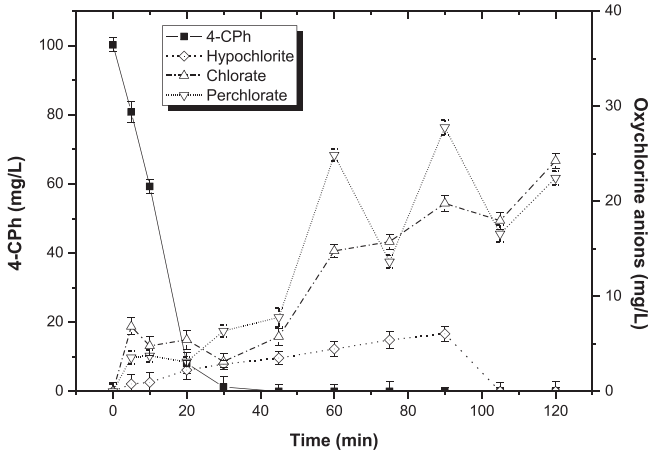

Fig. 11. Effect of E-peroxone on the temporary profiles of oxychlorine anions. *Reaction conditions:* $[Na_2SO_4]_o$= 0.05 M, $[4\text{-CPh}]_o$ = 100 mg·L^{-1}, V = 1.3 L, j = 0.060 A·cm^{-2}, F_{O3} = 10 mg/min, T = 20 ± 2 °C, pH_o= 7.0 ± 0.0.

to the oxidation of chloride ions by O_3 occurring faster than the plausible aforementioned chlorate reduction by H_2O_2. It is worth noticing that the consumer of O_3, i.e. the 4-chlorophenol, is exhausted after 75 min of treatment (see Fig. 3b) and this implies that after this time, the number of O_3 molecules available to oxidize other species like the chlorine ones, increases. This is even reflected in the appearance of O_3 after 90 min in Fig. 2b. It is important to note, in Fig. 9, that perchlorate is also being formed albeit at smaller concentration than in the electrochemical-based systems. Actually, the ozonation system is the only one where perchlorate is completely eliminated after 90 min of treatment. This can be explained based on the produced intermediary species. Small concentration of perchlorate ion has been related to the ozonation of ClO^- and ClO_3^-, while higher perchlorate concentration is expected when the ozonated molecule is ClO_2^- [45].

The above-mentioned reactions with ozone, take place due to the ozone oxidation potential E∘ (O_3 / O_2) = 2.07 V / SHE. These plausible reactions are summarized below [43,46],

$$2H^+ + 2Cl^- + O_3 \rightarrow O_2 + Cl_2 + H_2O \quad (35)$$

$$Cl^- + O_3 \rightarrow O_2 + ClO^- \quad (36)$$

$$ClO^- + O_3 \rightarrow O_2 + ClO_2^- \quad (37)$$

$$ClO_2^- + O_3 \rightarrow [ClO_2^{\bullet} + O_3^{\bullet -}] \rightarrow O_2 + ClO_3^- \quad (38)$$

$$ClO_3^- + O_3 \rightarrow O_2 + ClO_4^- \quad (39)$$

$$H_2O + Cl_2 + 5O_3 \rightarrow 2ClO_3^- + 5O_2 + 2H^+ \quad (40)$$

Regarding EO and EP, the anodic oxidation of chlorine species is undeniable [47] and leads to a higher accumulated concentration of ClO_4^- (see Figs. 10–11), than when only ozone is applied. In the electrochemical systems, in addition to reactions 35-40, Cl^- is progressively oxidized at the anode (BDD) to Cl_2 (reaction 41) and higher oxychlorine anions (reaction 42) [48] like chlorite (ClO_2^-), chlorate (ClO_3^-), perchlorate (ClO_4^-), hypochlorous acid/hypochlorite ($HOCl/OCl^-$). Actually, previous research suggests that BDD electrodes form twice faster perchlorates (ClO_4^-) than other electrodes, i.e. Pt, IrO_2, IrO_2, RuO_2.

$$2Cl^- \rightarrow Cl_2 + 2e^- \quad (41)$$

$$Cl^- \rightarrow HOCl/OCl^- \rightarrow ClO_2^- \rightarrow ClO_3^- \rightarrow ClO_4^- \quad (42)$$

The sequence shown by Eq. 42 is possible thanks to the hydroxyl radicals produced at the BDD surface and the following sequence of reactions proceeds,

$$Cl^- + HO^{\bullet} \rightleftharpoons HClO^{\bullet -} \rightleftharpoons Cl^{\bullet} + OH^- \quad (43)$$

$$Cl^- + Cl^{\bullet} \rightleftharpoons Cl_2^{\bullet -} \quad (44)$$

$$Cl^- + 6HO^{\bullet} \rightarrow ClO_3^- + 3H_2O \quad (45)$$

$$Cl^- + 8HO^{\bullet} \rightarrow ClO_4^- + 4H_2O \quad (46)$$

The production of chlorine radical by reaction 44, also allows the further participation of O_3 in the following reactions [43],

$$Cl_2^{\bullet -} + O_3 \rightarrow O_2 + ClO^{\bullet} + Cl^- \quad (47)$$

$$ClO^{\bullet} + ClO^{\bullet} \rightarrow Cl_2O_2 \quad (48)$$

$$Cl_2O_2 + H_2O \rightarrow 2H^+ + Cl^- + ClO_3^- \quad (49)$$

Species such as Cl_2O_2 and $ClO_2^{\bullet}$ have been considered instable during the degradation process since they are easily oxidized to species such as ClO_3^- [49] and this is the reason for not applying an analytical method to identify such oxychlorine compounds. In addition, the production of chlorate has been reported to be favored during EO and using sodium sulfate as anolyte. This phenomenon has been ascribed to the activation of the sulfate anions at the BDD anode, which can also react with oxychlorine radicals like $ClO_2^{\bullet}$ and then produce ClO_3^- [50]. Concomitantly, H_2O_2 (produced at the cathode) may react with the chlorinated species. This reaction can be either of reduction or oxidation, depending on the solution pH [51].

$$Cl^- + H_2O_2 \rightarrow ClO^- + H_2O \quad (51)$$

$$2ClO^- + H_2O_2 \rightarrow ClO_3^- + Cl^- + H_2O \quad (52)$$

$$ClO_3^- + H_2O_2 \rightarrow ClO_4^- + H_2O \quad (53)$$

$$2ClO^- + 2H_2O_2 \rightarrow 2Cl^- + 3O_2 + 4H^+ \quad (54)$$

$$2H^+ + 2ClO_3^- + H_2O_2 \rightarrow 2ClO_2 + 2H_2O + O_2 \quad (55)$$

Thus, it can be concluded that among the three assessed systems, the chlorine species are mostly reduced in the ozonation process, where only chlorine and chlorate were identified at the end of the treatment. It can be observed in all cases, that the moment where the oxychlorine ions accumulation slows down, coincides with a change in slope in the consumption of aromatic compounds, this was expected since the chlorinated aromatic compounds are the precursors of Cl^-.

It can be observed in Figs. 10–11, that during the first 5 min of reaction, appreciable amounts of ClO^-, ClO_3^- and ClO_4^- are observed only in the EP process and not in the EO process, despite the fact that ClO_4^- formation has been reported to be favored at high current densities during BDD electrolysis and that may be prevented using only small current densities to decrease the formation of $HO^{\bullet}$ and ClO_3^- and therefore the chance of their subsequent reaction to ClO_4^- in the diffusion layer of the BDD anode [52]. This supports the fact that, during the first five minutes of EP, the 4-CPh degradation is dominated by the molecular ozone attack rather than by hydroxyl radicals attack. These results also suggest, however, that the production of oxychlorine anions is dominated by hydroxyl radicals (reactions 43-46) rather than by O_3-based reactions. This coincides with the reaction sequence proposed by [11] albeit with a system free of organic molecules. In conclusion, in the electrochemical systems, the chlorinated species are predominantly transformed at the anode surface [43,47].

3.5. Toxicity

For each sample a toxicity bioassay with lettuce (*Lactuca sativa*) was conducted. This is a static toxicity test that is applied to establish the phytotoxic effects on seeds by monitoring their development during the first five days of growth (120 h).

Fig. 12 depicts the root elongation results in the control experiments. It can be observed that the lettuce seeds showed the highest percentage of germination (≥ 90%) in the control experiment with deionized water (CDI) and the average root elongation was 21.65 mm with a variation coefficient of 4.12, while in the other two control experiments, the root elongation was 17.53 mm and 5.84 mm for the control with sodium sulfate (CSS) and with zinc sulfate (positive control, PC), respectively. In these cases, the variation coefficient was 12.65 and 3.01. The average germination was 95%, 95% and 80% in the CDI, CSS and PC, respectively. These results reassure that there is not a toxicity effect in the negative controls (CDI and CSS) and there is toxicity in the control experiment with zinc sulfate. According to established criteria on phytotoxicity, a solution is considered toxic when the germination percentage is between 75% and 90% [53,54].

On the other hand, the inhibition of the radicle elongation is an indicator of sublethal toxicity [55], highly used to determine the quality of water and is considered more sensible towards toxicity than the seeds germination indicator. If the root elongation is lower than the 50% of the root elongation average in the control experiment, then it is concluded

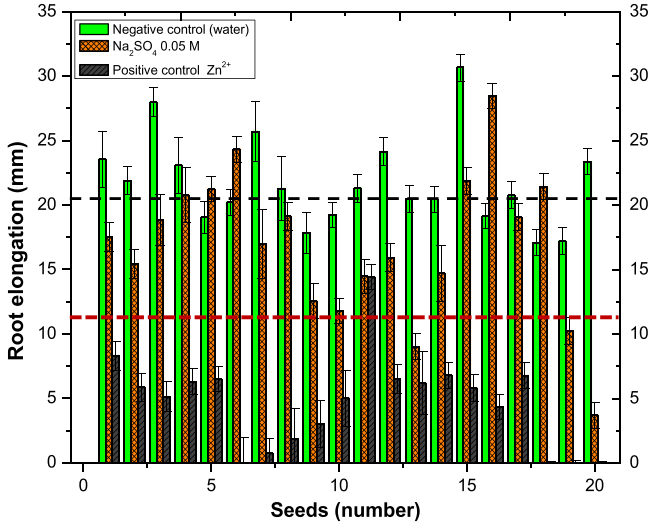

Fig. 12. Root elongation of *Lactuca sativa* seeds in the control experiments: deionized water, sodium sulfate (0.05 M) and $ZnSO_4.7\,H_2O$ (25 mg·L^{-1} of Zn^{2+}), pH= 7.0 ± 0.05.

that the solution is toxic [54]. The average of the root elongation in the CDI is indicated by the discontinuous black line in Fig. 12 while the red discontinuous line indicates the 50% of the root elongation average in the CDI. It can also be observed in Fig. 12, that the root elongation in 15% of the total seeds exposed to 0.05 M sodium sulfate solution, is lower than the 50% elongation of the CDI, indicating there is certain degree of toxicity exerted by the sodium sulfate. The toxicity of sodium sulfate has been previously reported by [54].

Fig. 13 shows the effect of treatment on germination index (GI). The values of RSG, RRG and corresponding relative standard deviation (RSD) to calculate this parameter, are provided in table S3 as supplementary material.

It can be observed in Fig. 13, that only the EP process allows the complete toxicity elimination from the treated solution after 105 min of reaction (GI > 90%). At the same time, the capacity of toxicity removal by EO is not very different from that attained with O_3, since with the former a GI = 30% is attained and GI = 20% with the latter. In the case of ozonation, to establish the species that are contributing the most to the observed toxicity, Figs. 2b, 3a, 3b, 8 and 9 are analyzed. In these figures, it can be observed that the remained compounds are mainly oxalic, succinic and formic acids (Fig. 3a), chloride (Fig. 8) and chlorate (Fig. 9). However, the concentration of both is lower than in EP (Figs. 8 and 11) where toxicity was the lowest, and therefore it can be inferred that chlorate does not contribute importantly to toxicity at the remained concentration of 12.5 $mg{\cdot}L^{-1}$. Thus, although chlorate has been recognized as a toxic specie to some plants [56], it can be concluded that in the case of ozonation, this toxicity can be ascribed to the produced carboxylic acids that were not further oxidized.

In EO, the main reason for the moderate toxicity at the end of treatment (120 min) are oxalic and formic acids (see Fig. 5a) as well as the unconsumed H_2O_2. This in concordance with that reported by [52]. At this point, however, the presence of persulfates cannot be discarded, and these might also be responsible for the toxicity increase observed after 75 min of EO treatment. In both processes, EO and EP, the presence of persulfates might be the result of sulfates oxidation [54]. In the case of EP, however, the produced persulfates could be activated and transformed to sulfate anions and hydroxyl radicals because of the produced alkaline conditions after 75 min of treatment [57]. According to these researchers, the persulfate anion undergoes hydrolysis and produces hydroperoxide (OH_2^-) and sulfate anions under alkaline conditions. Then hydroperoxide can also reduce persulfate to produce sulfate anions and radicals, superoxide radicals and protons. The reported global reaction is [54,57],

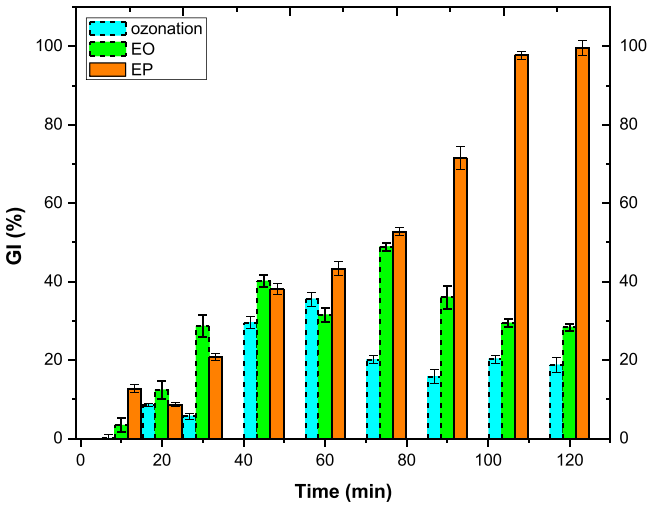

Fig. 13. Effect of type of treatment on germination index percentage (GI%) of *Lactuca sativa* seeds. Where: (L) is Low toxicity, (M) is Moderate toxicity and (H) is High toxicity or maximum phytotoxicity.

$$2S_2O_8^{2-} + 2H_2O \rightarrow 3SO_4^{2-} + SO_4^{\bullet-} + O_2^{\bullet-} + 4H^+ \quad (56)$$

Then, the produced sulfate and superoxide radicals can contribute to the production of hydroxyl radicals and sulfate anions via the following reactions,

$$SO_4^{\bullet-} + OH^- \rightarrow SO_4^{2-} + OH^{\bullet} \quad (57)$$

$$OH^{\bullet} + O_2^{\bullet-} \rightarrow O_2 + OH^- \quad (58)$$

$$SO_4^{\bullet-} + O_2^{\bullet-} \rightarrow SO_4^{2-} + O_2 \quad (59)$$

Although the phytotoxicity effects of sodium sulfate over *Lactuca sativa* have been documented [54], the toxicity of this salt is much lower (EC(48 h)= 2564 $mg{\cdot}L^{-1}$) than that of persulfates towards *Daphnia magna*, EC(48 h)= 133 $mg{\cdot}L^{-1}$ [54]. Thus, in the case of EP, the observed increase in pH after 75 min and the presence of O_3 helps to produce hydroperoxide via reaction 12. This anion is also the conjugated base of hydrogen peroxide and therefore its concentration will increase with pH, since the pKa of H_2O_2 is 11.75.

In EO, the toxic effect of chlorate and perchlorate at the remained concentrations of 25 and 23 $mg{\cdot}L^{-1}$, respectively, can be ruled out since they are, again, lower than those with the EP process where a low toxicity was determined at the end of treatment. This is in concordance with that published by Cook 1937 [58], who reported that 2500 $mg{\cdot}L^{-1}$ of perchlorate was the lethal dose to four different plants. This is two orders of magnitude higher than the concentrations obtained in this study. It is also worth pointing out that the USEPA [59] established a reference dose (RfD) of 0.0007 $mg{\cdot}kg^{-1}{\cdot}d^{-1}$ of perchlorate, equivalent to 24.5 $\mu g{\cdot}L^{-1}$ in drinking water [60].

Thus, it can be concluded that among the studied processes, only the EP treatment is able to eliminate the phytotoxicity effects of the 4-CPh solution with a zero toxicity after treatment.

3.6. Proposed pathway for the 4-CPh degradation by E-peroxone process

Based on the above discussion, in the first minutes of reaction (t < 5 min), the expected oxidant species would be molecular O_3, $HO^{\bullet}$ radicals at the anode, sulfate radicals at the anodic surface and persulfates. According to literature [29], O_3 induces dichlorination. In this case, and according to Fig. 8, this occurs faster by $HO^{\bullet}$ attack than by O_3. This may be the reason for detecting 4-chlorocatechol in much lower concentration in the electrochemical treatments than in O_3. Thus, in Fig. 14 two main routes of oxidation are distinguished, one conducted by the molecular attack of ozone that provokes the cleavage of the aromatic ring producing dicarboxylic acids that are readily oxidized by O_3 via a Criegee's mechanism [29]. This is supported by the appearance of maleic, fumaric, oxalic and formic acids since the first five minutes of treatment (Fig. 7a) which also led to a rapid decrease of pH (Fig. 6b). Therefore, although there are other oxidizing agents, the EP becomes predominant and this was also demonstrated by the synergy coefficient (0.31). This implies that despite the other oxidizing agents, the other route of reaction indicated in Fig. 14 is dominated by $HO^{\bullet}$. In this route, $HO^{\bullet}$ induces dichlorination and phenol and catechol appear. Later hydroxylation on the Carbon (C-4)-position of phenol led to hydroquinone which is subsequently dehydrogenated to p-Benzoquinone [61]. A parallel $HO^{\bullet}$ attack on Carbon (C-4)-position of 4-CPh also yields hydroquinone with loss of Cl^- [29]. The oxidation of benzoquinone, after the ring opening, led to the formation of aliphatic carboxylic acids such as maleic, malonic, succinic and fumaric acids, which were degraded to oxalic acid, acetic acid and formic acid [30]. The final products of mineralization were carbon dioxide, water and chloride.

4. Conclusions

H_2O_2 is in-situ produced when degrading 4-Chlorophenol via EP, EO

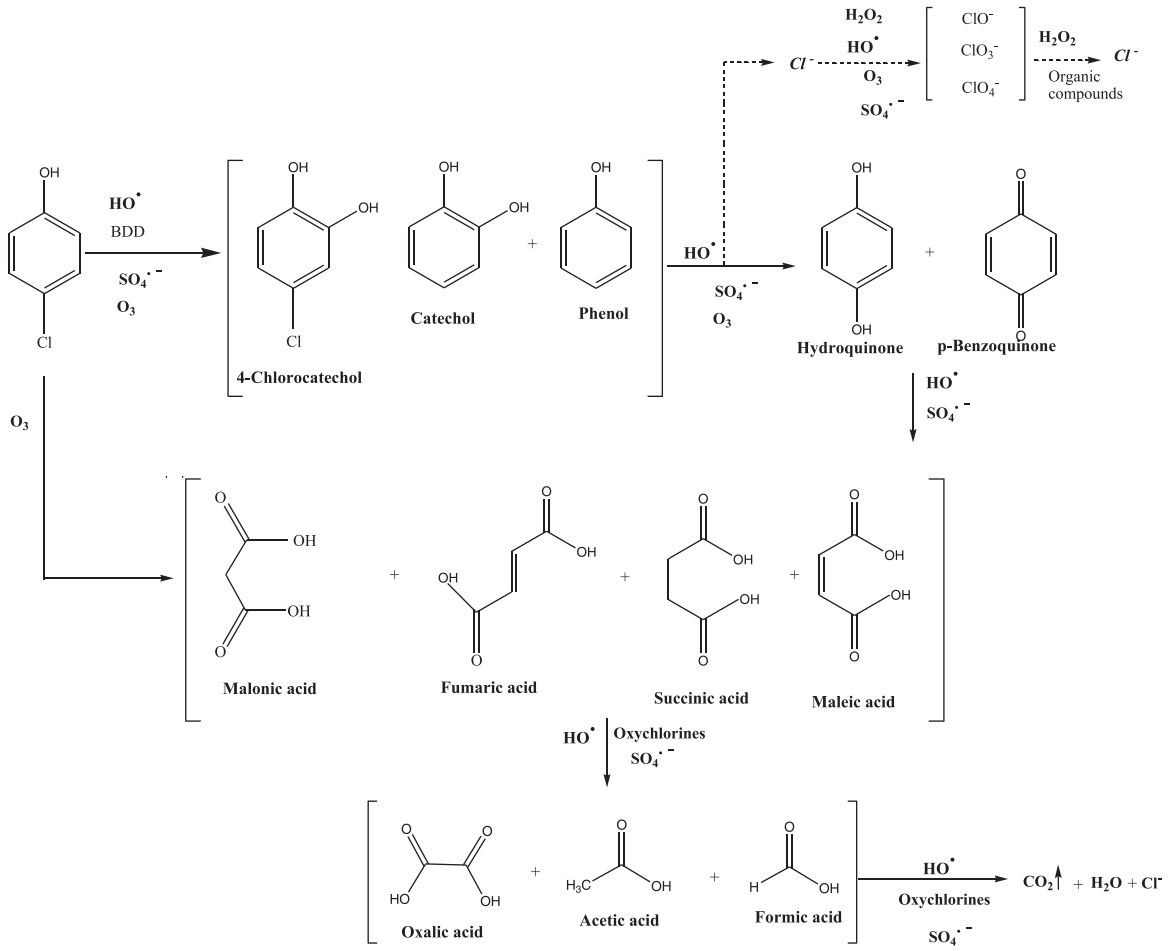

Fig. 14. Proposed 4-CPh degradation pathway by E-peroxone process (EP). Reaction conditions: $[Na_2SO_4]_o$= 0.05 M, $[4\text{-CPh}]_o$ = 100 mg·L^{-1}, V = 1.3 L, j = 0.060 A·cm^{-2}, F_{O3} = 10 mg/min, T = 20 ± 2 °C, pH_o= 7.0 ± 0.05.

or O_3. During the EP process, 4-CPh was rapidly destructed by molecular O_3 in the bulk solution and by the produced HO•. After a reaction time of 120 min, EP was found to be the only process that leads to the complete mineralization of 4-CPh and phytotoxicity removal. At the same reaction time, the mineralization reached by EO and O_3 was 93% and 40%, respectively. The calculated synergy coefficient for the EP was 0.31 at initial pH= 7, while the mineralization current efficiency percentage (MCE%) and the energy consumption (EC) were 12.24% and 11.48%, 2.84 and 2.31 kW·h^{-1}, for EP and EO, respectively. The germination percentage of *Lactuca sativa,* was 100%, 30% and 20%, at the end of EP, EO and O_3, respectively. This indicates that phytotoxicity, was only eliminated with EP. In the three processes, O_3 and/or H_2O_2 are in-situ produced. The HO• production is rather limited during ozonation and intensified by the electrochemical process. Thus, the carboxylic acids that are resistant to be oxidized by molecular O_3, are effectively mineralized by HO• produced from the multiple sources (e.g. H_2O oxidation at the BDD anode, sulfate radicals and O_3 decomposition at alkaline pH) in the EP system. The maximum chloride and oxychlorine anions concentration vary according to the following order EP>EO>O_3. Hypochlorite formation is not detected during the ozonation process. This process does not favor perchlorate formation neither.

In the O_3 and EO processes, the observed toxicity at the end of treatment can be ascribed to the presence of carboxylic acids, unconsumed H_2O_2, sulfates and persulfates (in EO).

CRediT authorship contribution statement

Deysi Amado Piña (DAP), Rubi Romero (RR) and Patricia Balderas Hernandez (PBH) acquired and analyzed the data. DAP and Carlos Barrera (CB) drafted the manuscript. Gabriela Roa (GR) and Reyna Natividad (RN) conceptualized and designed the study, revised the manuscript critically for important intellectual content. All authors approved the version of the manuscript to be published.

Declaration of Competing Interest

The authors declare that they have no known competing financial interests or personal relationships that could have appeared to influence the work reported in this paper.

Acknowledgments

The authors wish to acknowledge the support given by COMECYT and CONACYT. The technical support of Citlalit Martínez Soto is also acknowledged.

Appendix A. Supporting information

Supplementary data associated with this article can be found in the online version at doi:10.1016/j.jece.2022.108148.

References

[1] J.P. Pocostales, M.M. Sein, W. Knolle, C. von Sonntag, T.C. Schmidt, Degradation of ozone-refractory organic phosphates in wastewater by ozone and ozone/hydrogen peroxide (peroxone): the role of ozone consumption by dissolved organic matter, Environ. Sci. Technol. 44 (2010) 8248–8253, https://doi.org/10.1021/es1018288.

[2] J.M. Poyatos, M.M. Muñio, M.C. Almecija, J.C. Torres, E. Hontoria, F. Osorio, Advanced oxidation processes for wastewater treatment: state of the art, Water Air Soil Pollut. 205 (2009) 187–204, https://doi.org/10.1007/s11270-009-0065-1.

[3] U.Von Gunten, Ozonation of drinking water: Part I. Oxidation kinetics and product formation, Water Res 37 (2003) 1443–1467, https://doi.org/10.1016/S0043-1354(02)00457-8.

[4] S. Esplugas, J. Giménez, S. Contreras, E. Pascual, M. Rodríguez, Comparison of different advanced oxidation processes for phenol degradation, Water Res 36 (2002) 1034–1042, https://doi.org/10.1016/S0043-1354(01)00301-3.

[5] P.J. Espinoza-Montero, P. Alulema-Pullupaxi, B.A. Frontana-Uribe, C.E. Barrera-Diaz, Electrochemical production of hydrogen peroxide on Boron-Doped diamond (BDD) electrode, Curr. Opin. Solid State Mater. Sci. 26 (2022), 100988, https://doi.org/10.1016/j.cossms.2022.100988.

[6] B. Bakheet, S. Yuan, Z. Li, H. Wang, J. Zuo, S. Komarneni, Y. Wang, Electro-peroxone treatment of Orange II dye wastewater, Water Res 47 (2013) 6234–6243, https://doi.org/10.1016/j.watres.2013.07.042.

[7] Y. Li, W. Shen, S. Fu, H. Yang, G. Yu, Y. Wang, Inhibition of bromate formation during drinking water treatment by adapting ozonation to electro-peroxone process, Chem. Eng. J. 264 (2015) 322–328, https://doi.org/10.1016/j.cej.2014.11.120.

[8] O.M. Cornejo, M. Ortiz, Z.G. Aguilar, J.L. Nava, Degradation of Acid Violet 19 textile dye by electro-peroxone in a laboratory flow plant, Chemosphere 271 (2021), 129804, https://doi.org/10.1016/J.CHEMOSPHERE.2021.129804.

[9] O.M. Cornejo, J.L. Nava, Incineration of the antibiotic chloramphenicol by electro-peroxone using a smart electrolyzer that produces H2O2 through electrolytic O2, Sep. Purif. Technol. 282 (2022), 120021, https://doi.org/10.1016/J.SEPPUR.2021.120021.

[10] G. Santana-Martínez, G. Roa-Morales, L. Gómez-Olivan, E. Peralta-Reyes, R. Romero, R. Natividad, Downflow bubble column electrochemical reactor (DBCER): In-situ production of H2O2 and O3 to conduct electroperoxone process, J. Environ. Chem. Eng. 9 (2021), 105148, https://doi.org/10.1016/j.jece.2021.105148.

[11] Z. Lin, W. Yao, Y. Wang, G. Yu, S. Deng, J. Huang, B. Wang, Perchlorate formation during the electro-peroxone treatment of chloride-containing water: effects of operational parameters and control strategies, Water Res 88 (2016) 691–702, https://doi.org/10.1016/j.watres.2015.11.005.

[12] O.M. Cornejo, J.L. Nava, Mineralization of the antibiotic levofloxacin by the electro-peroxone process using a filter-press flow cell with a 3D air-diffusion electrode, Sep. Purif. Technol. 254 (2021), 117661, https://doi.org/10.1016/J.SEPPUR.2020.117661.

[13] C. Qu, G.S. Soomro, N. Ren, D. Wei Liang, S. Fu Lu, Y. Xiang, S. Jun Zhang, Enhanced electro-oxidation/peroxone (in situ) process with a Ti-based nickel-antimony doped tin oxide anode for phenol degradation, J. Hazard. Mater. 384 (2020), 121398, https://doi.org/10.1016/j.jhazmat.2019.121398.

[14] C. Qu, S. Lu, D. Liang, S. Chen, Y. Xiang, S. Zhang, Simultaneous electro-oxidation and in situ electro-peroxone process for the degradation of refractory organics in wastewater, J. Hazard. Mater. 364 (2019) 468–474, https://doi.org/10.1016/j.jhazmat.2018.10.073.

[15] Z. Lang, M. Zhou, Q. Zhang, X. Yin, Y. Li, Comprehensive treatment of marine aquaculture wastewater by a cost-effective flow-through electro-oxidation process, Sci. Total Environ. 722 (2020), 137812, https://doi.org/10.1016/j.scitotenv.2020.137812.

[16] X. Li, Y. Wang, S. Yuan, Z. Li, B. Wang, J. Huang, S. Deng, G. Yu, Degradation of the anti-inflammatory drug ibuprofen by electro-peroxone process, Water Res. 63 (2014) 81–93, https://doi.org/10.1016/j.watres.2014.06.009.

[17] Z. Li, S. Yuan, C. Qiu, Y. Wang, X. Pan, J. Wang, C. Wang, J. Zuo, Effective degradation of refractory organic pollutants in landfill leachate by electro-peroxone treatment, Electrochim. Acta 102 (2013) 174–182, https://doi.org/10.1016/j.electacta.2013.04.034.

[18] X. Chen, G. Chen, Fabrication and application of Ti/BDD for wastewater treatment, Synth. Diam. Film. Prep. Electrochem. Charact. Appl. (2011) 353–371, https://doi.org/10.1002/9781118062364.ch15.

[19] A.R. Ribeiro, O.C. Nunes, M.F.R. Pereira, A.M.T. Silva, An overview on the advanced oxidation processes applied for the treatment of water pollutants de fi ned in the recently launched Directive 2013 / 39 / EU, Environ. Int. 75 (2015) 33–51, https://doi.org/10.1016/j.envint.2014.10.027.

[20] G. Eisenberg, Colorimetric determination of hydrogen peroxide, Ind. Eng. Chem. Anal. Ed. 15 (1943) 327–328, https://doi.org/10.1021/i560117a011.

[21] H. Bader, J. Hoigné, Determination of ozone in water by the indigo method, Water Res 15 (1981) 449–456, https://doi.org/10.1016/0043-1354(81)90054-3.

[22] D.V. Girenko, A.A. Gyrenko, N.V. Nikolenko, Potentiometric determination of chlorate impurities in hypochlorite solutions, Int. J. Anal. Chem. 2019 (2019) 1–7, https://doi.org/10.1155/2019/2360420.

[23] S. de C. y F. Industrial, Water Qualitty- Total Chlorine Determination Iodometric Method, in: NMX-AA-100–1987, MEXICO, 1987: pp. 4–7.

[24] E.T. Urbansky, Perchlorate chemistry: implications for analysis and remediation, Bioremediat. J. 2 (1998) 81–95, https://doi.org/10.1080/10889869891214231.

[25] N.J. Hoekstra, T. Bosker, E.A. Lantinga, Effects of cattle dung from farms with different feeding strategies on germination and initial root growth of cress (Lepidium sativum L.), Agric. Ecosyst. Environ. 93 (2002) 189–196, https://doi.org/10.1016/S0167-8809(01)00348-6.

[26] D. Amado-Piña, G. Roa-Morales, C. Barrera-Díaz, P. Balderas-Hernandez, R. Romero, E. Martín del Campo, R. Natividad, Synergic effect of ozonation and electrochemical methods on oxidation and toxicity reduction: Phenol degradation, Fuel 198 (2017) 82–90, https://doi.org/10.1016/j.fuel.2016.10.117.

[27] C.C.-P. Bohórquez, P.-Echeverry, Assessment of Lactuca sativa and Selenastrum capricornutum Like Indicators of water Toxicity, Univ. Sci. 12 (2007) 83–98.

[28] U. von Gunten, Ozonation of drinking water: Part I. Oxidation kinetics and product formation, Water Res 37 (2003) 1443–1467, https://doi.org/10.1016/S0043-1354(02)00457-8.

[29] T. Poznyak, R. Tapia, J. Vivero, I. Chairez, Effect of pH to the decomposition of aqueous phenols mixture by ozone, J. Mex. Chem. Soc. 50 (2006) 28–35.

[30] J.B. Fernando, Ozone Reaction Kinetics for Water and Wastewater Systems, Lewis Publishers, Washington, D.C, 2003.

[31] Y. Pi, L. Zhang, J. Wang, The formation and influence of hydrogen peroxide during ozonation of para-chlorophenol, J. Hazard. Mater. 141 (2007) 707–712, https://doi.org/10.1016/j.jhazmat.2006.07.032.

[32] A.A.A. El-Raady, T. Nakajima, Decomposition of carboxylic acids in water by O 3, O 3 /H 2 O 2, and O 3 /catalyst, Ozone Sci. Eng. 27 (2005) 11–18, https://doi.org/10.1080/01919510590908922.

[33] H. Tomiyasu, H. Fukutomi, G. Gordon, Kinetics and mechanism of ozone decomposition in basic aqueous solution, Inorg. Chem. 24 (1985) 2962–2966, https://doi.org/10.1021/ic00213a018.

[34] G.C. Christos Comninellis, Electrochemistry for the Environment, Springer New York, New York, NY, 2010, https://doi.org/10.1007/978-0-387-68318-8.

[35] P. Frangos, W. Shen, H. Wang, X. Li, G. Yu, S. Deng, J. Huang, B. Wang, Y. Wang, Improvement of the degradation of pesticide deethylatrazine by combining UV photolysis with electrochemical generation of hydrogen peroxide, Chem. Eng. J. 291 (2016) 215–224, https://doi.org/10.1016/j.cej.2016.01.089.

[36] H. Wang, B. Bakheet, S. Yuan, X. Li, G. Yu, S. Murayama, Y. Wang, Kinetics and energy efficiency for the degradation of 1,4-dioxane by electro-peroxone process, J. Hazard. Mater. 294 (2015) 90–98, https://doi.org/10.1016/j.jhazmat.2015.03.058.

[37] J. Lee, U. Von Gunten, J.H. Kim, Persulfate-based advanced oxidation: critical assessment of opportunities and roadblocks, Environ. Sci. Technol. 54 (2020) 3064–3081, https://doi.org/10.1021/acs.est.9b07082.

[38] L. Chen, C. Lei, Z. Li, B. Yang, X. Zhang, L. Lei, Electrochemical activation of sulfate by BDD anode in basic medium for efficient removal of organic pollutants, Chemosphere 210 (2018) 516–523, https://doi.org/10.1016/j.chemosphere.2018.07.043.

[39] G. Asgari, A. Seid-mohammadi, A. Rahmani, M.T. Samadi, M. Salari, S. Alizadeh, D. Nematollahi, Diuron degradation using three-dimensional electro-peroxone (3D/E-peroxone) process in the presence of TiO2/GAC: application for real wastewater and optimization using RSM-CCD and ANN-GA approaches, Chemosphere 266 (2021), 129179, https://doi.org/10.1016/j.chemosphere.2020.129179.

[40] E. Peralta, M. Ruíz, G. Martínez, J. Mentado-Morales, L.G. Zárate, M.E. Cordero, M. A. Garcia-Morales, R. Natividad, A. Regalado-Méndez, Degradation of 4-chloro-phenol in a batch electrochemical reactor using BDD electrodes, Int. J. Electrochem. Sci. 1321 (2018) 4625–463905, https://doi.org/10.20964/2018.05.21.

[41] J.-L. Chen, G.-C. Chiou, C.-C. Wu, Electrochemical oxidation of 4-chlorophenol with granular graphite electrodes, Desalination 264 (2010) 92–96, https://doi.org/10.1016/j.desal.2010.07.009.

[42] G. Santana-martínez, G. Roa-morales, E. Martin, R. Romero, B.A. Frontana-uribe, R. Natividad, Electrochimica Acta Electro-Fenton and Electro-Fenton-like with in situ electrogeneration of H_2O_2 and catalyst applied to 4-chlorophenol mineralization, Electrochim. Acta 195 (2016) 246–256, https://doi.org/10.1016/j.electacta.2016.02.093.

[43] A.V. Levanov, O.Y. Isaikina, R.B. Gasanova, A.S. Uzhel, V.V. Lunin, Kinetics of chlorate formation during ozonation of aqueous chloride solutions, Chemosphere 229 (2019) 68–76, https://doi.org/10.1016/j.chemosphere.2019.04.105.

[44] S. Cotillas, J. Llanos, M.A. Rodrigo, P. Cañizares, Use of carbon felt cathodes for the electrochemical reclamation of urban treated wastewaters, Appl. Catal. B Environ. 162 (2015) 252–259, https://doi.org/10.1016/j.apcatb.2014.07.004.

[45] N. Kang, W.A. Jackson, P.K. Dasgupta, T.A. Anderson, Perchlorate production by ozone oxidation of chloride in aqueous and dry systems, Sci. Total Environ. 405 (2008) 301–309, https://doi.org/10.1016/J.SCITOTENV.2008.07.010.

[46] M.S. Siddiqui, Chlorine-ozone interactions: formation of chlorate, Water Res 30 (1996) 2160–2170, https://doi.org/10.1016/0043-1354(96)00071-1.

[47] Z. Lin, W. Yao, Y. Wang, G. Yu, S. Deng, J. Huang, B. Wang, Perchlorate formation during the electro-peroxone treatment of chloride-containing water: effects of operational parameters and control strategies, Water Res 88 (2016) 691–702, https://doi.org/10.1016/j.watres.2015.11.005.

[48] O. Azizi, D. Hubler, G. Schrader, J. Farrell, B.P. Chaplin, Mechanism of Perchlorate Formation on Boron-Doped Diamond Film Anodes, Environ. Sci. Technol. 45 (2011) 10582–10590, https://doi.org/10.1021/es202534w.

[49] N. Huang, W.L. Wang, Z. Bin Xu, M.Y. Lee, Q.Y. Wu, H.Y. Hu, A study of synergistic oxidation between ozone and chlorine on benzalkonium chloride degradation: reactive species and degradation pathway, Chem. Eng. J. 382 (2020), 122856, https://doi.org/10.1016/J.CEJ.2019.122856.

[50] J. Radjenovic, M. Petrovic, Removal of sulfamethoxazole by electrochemically activated sulfate: implications of chloride addition, J. Hazard. Mater. 333 (2017) 242–249, https://doi.org/10.1016/j.jhazmat.2017.03.040.

[51] B. Rao, T.A. Anderson, A. Redder, W.A. Jackson, Perchlorate formation by ozone oxidation of aqueous chlorine/oxy-chlorine species: role of ClxOy radicals, Environ. Sci. Technol. 44 (2010) 2961–2967, https://doi.org/10.1021/es903065f.

[52] S.M.L. d O. Marcionilio, D.M. Araújo, T. de, V. Nascimento, C.A. Martínez-Huitle, J. J. Linares, Evaluation of the toxicity reduction of an ionic liquid solution electrochemically treated using BDD films with different sp3/sp2 ratios,

Electrochem. Commun. 118 (2020), 106792, https://doi.org/10.1016/j.elecom.2020.106792.
[53] M.G. Bagur-González, C. Estepa-Molina, F. Martín-Peinado, S. Morales-Ruano, Toxicity assessment using Lactuca sativa L. bioassay of the metal(loid)s As, Cu, Mn, Pb and Zn in soluble-in-water saturated soil extracts from an abandoned mining site, J. Soils Sediment. 11 (2011) 281–289, https://doi.org/10.1007/s11368-010-0285-4.
[54] M.T. Montañés, M. García-Gabaldón, L. Roca-Pérez, J.J. Giner-Sanz, J. Mora-Gómez, V. Pérez-Herranz, Analysis of norfloxacin ecotoxicity and the relation with its degradation by means of electrochemical oxidation using different anodes, Ecotoxicol. Environ. Saf. 188 (2020), 109923, https://doi.org/10.1016/j.ecoenv.2019.109923.
[55] A.N.A. Heberle, M.E.P. Alves, S.W. da Silva, C.R. Klauck, M.A.S. Rodrigues, A. M. Bernardes, Phytotoxicity and genotoxicity evaluation of 2,4,6-tribromophenol solution treated by UV-based oxidation processes, Environ. Pollut. 249 (2019) 354–361, https://doi.org/10.1016/j.envpol.2019.03.057.
[56] R. Borges, E.C. Miguel, J.M.R. Dias, M. Da Cunha, R.E. Bressan-Smith, J.G. De Oliveira, G.A. De Souza Filho, Ultrastructural, physiological and biochemical analyses of chlorate toxicity on rice seedlings, Plant Sci. 166 (2004) 1057–1062, https://doi.org/10.1016/j.plantsci.2003.12.023.
[57] O.S. Furman, A.L. Teel, R.J. Watts, Mechanism of base activation of persulfate, Environ. Sci. Technol. 44 (2010) 6423–6428, https://doi.org/10.1021/es1013714.
[58] W.H. Cook, Chemical weed killers: V. Relative toxicity of selected chemicals to plants grown in culture solution, and the use of relative growth rate as a criterion of toxicity, Can. J. Res. 15c (1937) 520–537, https://doi.org/10.1139/cjr37c-039.
[59] C.C.-P. Bohórquez, P.-Echeverry, Assessment of Lactuca sativa and Selenastrum capricornutum Like Indicators of water Toxicity, Univ. Sci. 12 (2007) 83–98.
[60] R. Calderón, P. Palma, D. Parker, M. Escudey, Capture and accumulation of perchlorate in lettuce. Effect of genotype, temperature, perchlorate concentration, and competition with anions, Chemosphere 111 (2014) 195–200, https://doi.org/10.1016/j.chemosphere.2014.03.027.
[61] C. von Sonntag, U. von Gunten, Chemistry of Ozone in Water and Wastewater Treatment: From Basic Principles to Applications, IWA Publishing Alliance House, London-New York, 2015, https://doi.org/10.2166/9781780400839.